1. Literature study

1.1. Introduction

Vanadium recovery in the electro-aluminothermic process is influenced by a number of factors relating to the production process, for instance raw materials handling, flux additions, temperature control and tapping procedure. Because of the high selling price of the final product, is it essential to identify and investigate the relative effect of each factor on the vanadium recovery, aiming to optimize the process. The most important recovery-linked factors that still await clarification can, if possible, be addressed by performing experiments. The objective of the following discussion is to provide background on some areas that were studied experimentally by the author.

1.2. Production of ferrovanadium

1.2.1. Introduction

Ferrovanadium represents today a group of vanadium compounds and alloys some of which do not even contain iron, but all of which serve the function of introducing vanadium into iron and steel. It is difficult to produce pure vanadium metal because vanadium readily reacts and absorbs oxygen, nitrogen and carbon. Furthermore the presence of impurities renders the vanadium metal brittle (Gupta,1992).

Ferrovanadium is produced by the reduction of vanadium bearing starter materials including slags, boiler residues, fly ash and vanadium oxides, using carbon, silicon or aluminium as reductant. The vanadium oxides can be in the form of V_2O_5, V_2O_4, V_2O_3 or mixtures of these oxides. The exothermicity of the reaction is a function of the level of vanadium oxidation and the concentration of each species in the raw material. This would therefore determine to what extent external energy is required. Depending on the production process and raw materials used, the concentration of vanadium in ferrovanadium generally ranges from 40 to 85 % by weight, and the industry classifies ferrovanadium into grades accordingly. Table 1 shows typical chemical specifications for commercial forms of ferrovanadium.

Alloy	Composition (Mass %)							
	V	C	N	Al	Si	P	S	Mn
50 –60 % ferrovanadium	50-60	0.2 max		2 max	1 max	0.05 max	0.05 max	
70 –80 % ferrovanadium	70-80			1 max	2.5 max	0.05 max	0.10 max	
80 % ferrovanadium	77-83	0.5 max		0.5 max	1.25 max	0.05 max	0.05 max	0.05 max
Carvan	82-86	10.5-14.5		0.1 max	0.1 max	0.05 max	0.10 max	
Ferrovanadium carbide	70-73	10-12			0.5 max	0.05 max	0.05 max	0.05 max
Ferrovan	42 min	0.85 max			7 max			4.5 max
Nitrovan	78-82	10-12	6 min	0.10 max	0.1 max	0.05 max	0.05 max	0.05 max

Table 1: Typical chemical compositions, with Fe as balance, for commercial forms of ferrovanadium (Gupta,1992).

The methods of producing ferrovanadium are discussed below

1.2.2. Carbothermic reduction

Reduction with carbon is conducted in a submerged-arc furnace. Carbon in the form of coke, coal, "char" or charcoal can be used. Carbothermic reduction is endothermic and so the process is energy intensive. Thus, successful production of ferrovanadium by carbon reduction of vanadium pentoxide requires the introduction of the furnace charge into the high temperature zone under strongly reducing conditions. The furnace usually has a rectangular cross section, using either two or three electrodes arranged in line. The electrodes create a high temperature reduction zone (Gupta,1992). The charge mainly consists of vanadium oxide, carbon source, steel scrap and fluxing agents.

The charge is fed into the high-energy reduction zone and ferrovanadium and slag accumulate below the arc and are tapped at 4-12h intervals (Hayward,1952).

A typical ferrovanadium composition for this process is as follows: 33-42 % V, 3-5 % Si, 3-3.5%C and balance Fe (Gupta,1992). The high residual carbon content in the alloy and the difficulty in regulating the carbon content have made carbothermic reduction in the arc furnace less attractive than alternative routes. The carbon reduction process is mainly used for the production of high C-grade ferrovanadium for example "Carvan" (85 %

Vanadium, 12 % Carbon, 2 % iron), used in applications where carbon and carbides are not detrimental.

The development of a falling film plasma reactor has changed the limited use of carbothermic reduction considerably. Plasma reactors enable endothermic reactions in carbothermic reduction to be carried out at very high temperatures, thus establishing higher yields. MacRae et al (1976) developed a falling film plasma reactor to produce ferrovanadium, shown in figure 1.

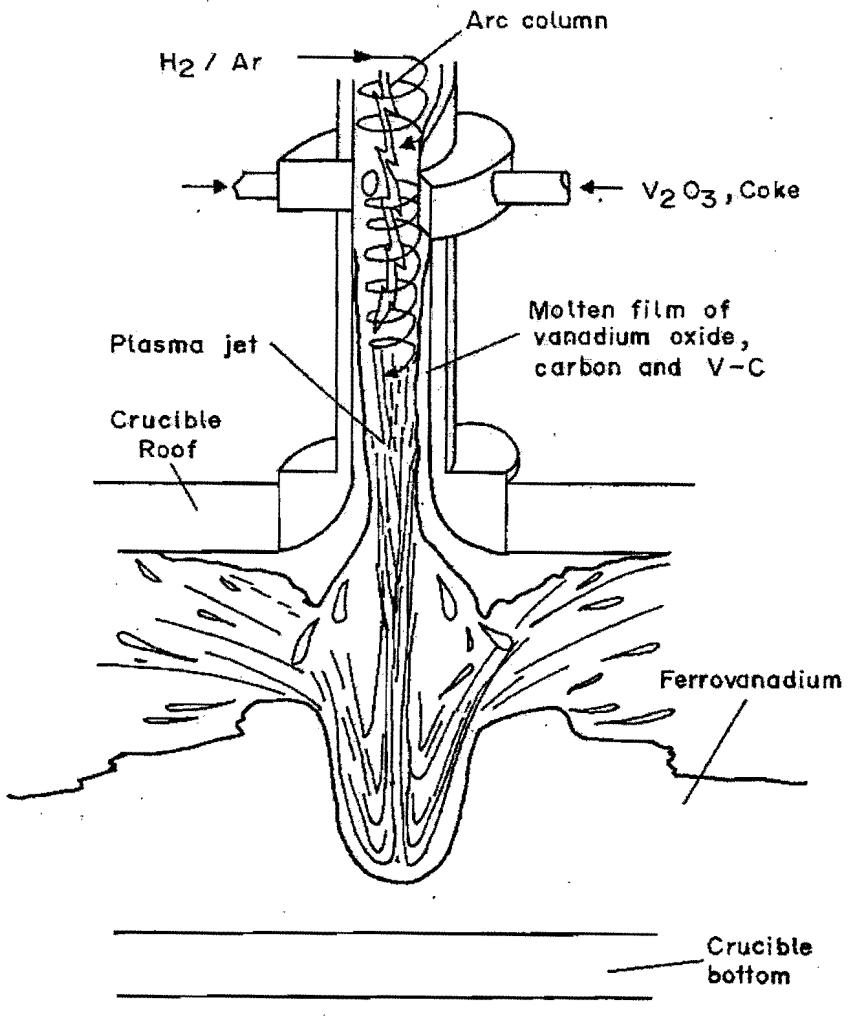

Figure 1: Falling film plasma reactor (Gupta,1992).

Vanadium oxide and coke fines are injected into the arc which is struck between a tungsten cathode and a tubular copper anode. The molten liquid flows down the anode wall into a receiving crucible. In essence the film enables intimate contact between the

reactants and the long residence time provides sufficient time for heat transfer, thus driving the reaction almost to completion. The product contains typically 42 % V, 53% Fe and 3 % C. Despite the good heat transfer to the reactants, the power consumption is still 3200 kWh/ton ferrovanadium produced.

1.2.3. Silicon reduction

In this route the reductant is a high-grade ferrosilicon containing 75% silicon. Silicon is not a powerful reducer of vanadium oxides; thus a two-stage process is required. Technical grade vanadium pentoxide is smelted to produce ferrovanadium containing about 30% vanadium with a considerable amount of residual silicon. According to Khodorovsky et al (1967), the slag composition is 50-55% CaO, 5-10% MgO, 28-30% SiO_2 and 0.5% V. The overall reaction can be represented by

$$2V_2O_5 + 5(Fe_{y/5}Si)_{alloy} + 10CaO = 4(Fe_{y/4}V)_{alloy} + 5Ca_2SiO_4 \qquad (1)$$

The primary metal is refined with vanadium pentoxide and lime in a second step and the secondary slag is returned as part of the charge to produce primary metal. Lower vanadium oxides such as V_2O_3 and VO interact with silica to form vanadium silicates, thus making the reduction process difficult and more complicated. As a result the slag traps some vanadium and the recovery rarely exceeds 75-80% (Gupta,1992).

1.2.4. Aluminium reduction

The reduction of vanadium oxide with aluminium can be further subdivided into the aluminothermic (thermit) and the electro-aluminothermic processes. The nature of the vanadium oxide used as input material governs the production route as is indicated in the next sections.

1.2.4.1. Reduction of vanadium oxides

The reduction of vanadium oxides by aluminium can be represented by the following set of reactions. (The heats of the reactions were calculated using correlations of

Kubaschewski et al. (1993) for enthalpy values at 298 K and 2073 K for the reactants and products respectively):

$$3V_2O_5 + 10Al \rightarrow 6V + 5Al_2O_3 \; ; \Delta H^\circ = -4.28 * 10^5 \text{ J/mol V} \quad (2)$$

$$3V_2O_4 + 8Al \rightarrow 6V + 4Al_2O_3 \; ; \Delta H^\circ = -2.37 * 10^5 \text{ J/mol V} \quad (3)$$

$$V_2O_3 + 2Al \rightarrow 2V + Al_2O_3 \; ; \Delta H^\circ = -9.25 * 10^4 \text{ J/mol V} \quad (4)$$

$$3VO + 2Al \rightarrow 3V + Al_2O_3 \; ; \Delta H^\circ = -1.52 * 10^4 \text{ J/mol V} \quad (5)$$

The enthalpy of the exothermic reaction can be used to predict whether the reaction releases enough energy to melt the metal and slag. The ratio of the heat of the reaction and the molecular weight of the products is generally used to determine the exothermicity of the reaction. If the ratio >4 500 J/gram, then the reaction is violent, under 2250 J/gram external supply of heat is necessary and between 2250 J/gram and 4500 J/gram the reaction develops in a controlled manner and external energy is not necessary (Yücel,1996). Only slag reaction 2 is sufficiently exothermic to obtain liquid metal given the very high melting temperature of ferrovanadium (typically 1750 °C).

1.2.4.2. Aluminothermic reduction

The process can be characterized by reaction 2. This reaction is strongly exothermic and once it has been initiated it can both melt the iron added to make the alloy and allow for effective separation of the alloy and the high aluminium slag. The aluminothermic reactor is presented in figure 2.

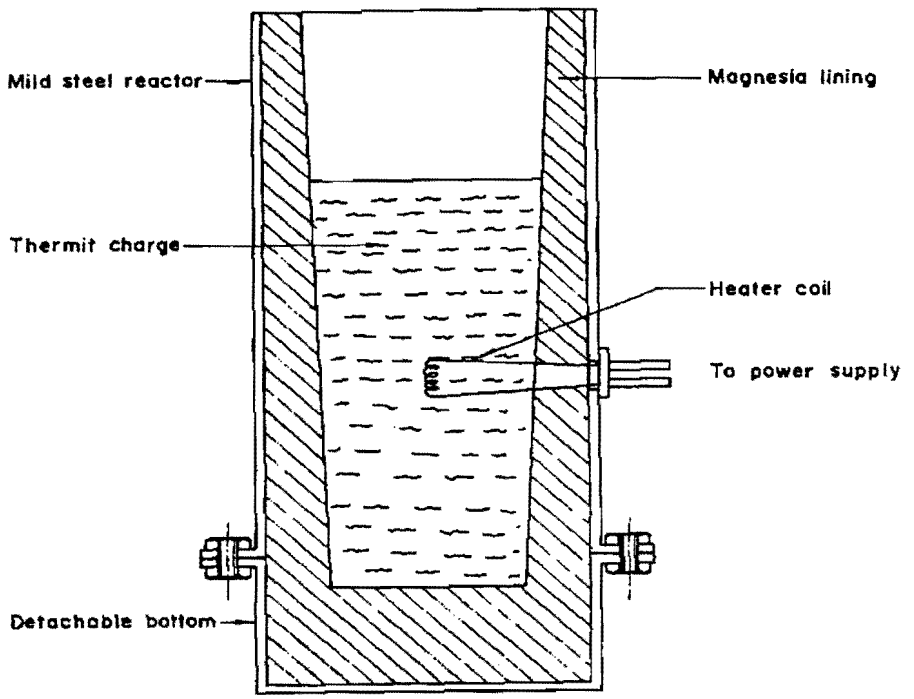

Figure 2: Aluminothermic reactor (Gupta,1992).

The charge mix consists mainly of V_2O_5, scrap iron, aluminium (particle size: 0.7 - 1.1 mm, Nyirfa[1985]) and lime. The materials are thoroughly mixed before being fed to the reactor. Two distinct smelting methods can be distinguished namely "the reverse reaction" and "feeded reaction" methods. In the feeded reaction method only part of the charge mix is fed to the reactor and then this is ignited. The remainder of the charge mix is fed progressively according to the speed of the reactions. The method requires well-trained operators. In the reverse reaction method the entire charge mix is loaded into the reactor and ignited in such a way that the reaction can proceed downwards. The heater coil is embedded in the mixture so that the reaction can be initiated remotely by passing a current through the coil. Once initiated the reaction proceeds to completion.

Adjusting the feed rate and the particle size of especially aluminium can control the rate of the feeded reaction. If the aluminium granules are too big the reaction interfaces are small resulting in slow and incomplete reactions. The rate of fusion of the initial charge increases with an increase of the specific surface area and with greater addition of aluminium shot. Figure 3 shows the effect of granule size and the amount of Al added on the rate of fusion of the charge. The rate of charge fusion determines the rate of the reduction process.

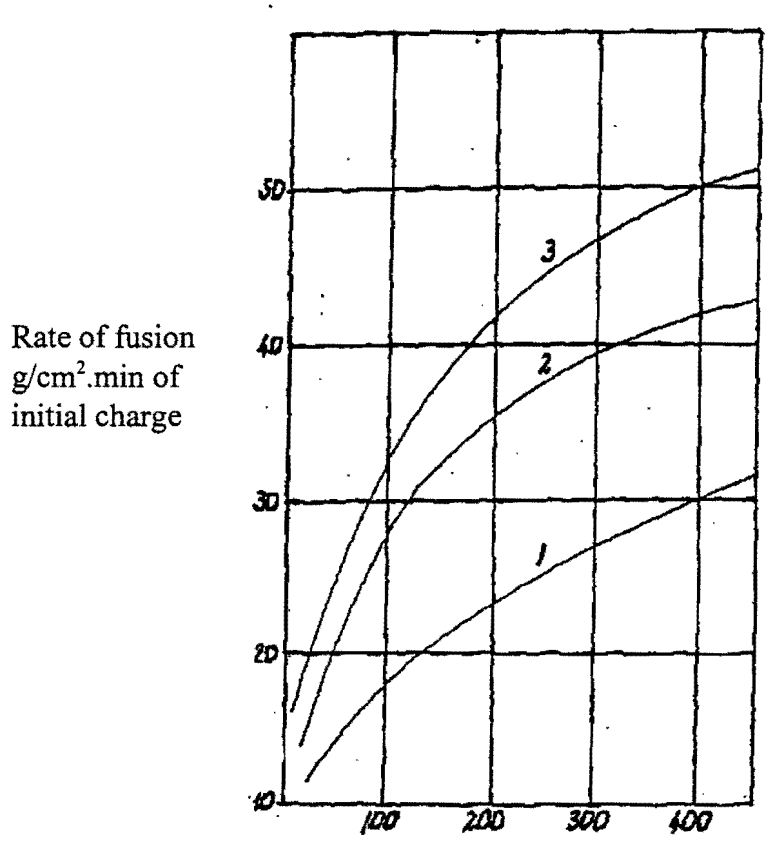

Figure 3: Effect of the amount of aluminium and of its specific surface area on the fusion rate of the charge (Nyirfa,1985). Curve 2 represents the stoichiometric amount of aluminium added. The other curves are where this amount is reduced by 20 % (Curve 1) and increased by 20 % (Curve3).

Large size granules cause increased amounts of large-size drops of alloy being trapped in the slag. Although the increase of aluminium above the stoichiometrically needed amount results in faster reactions and improves the vanadium recovery, it does increase the final Al content of the alloy. There are strict specifications set by the consumer regarding the aluminium content of the alloy, indicated by Table 1, thus necessitating the optimization of the recovery process by adjusting parameters influencing the vanadium distribution between slag and metal. One such parameter is the slag basicity. The slag basicity has a dual influence on the vanadium recovery in the sense that it influences the vanadium activity coefficient and the slag viscosity, which in turn has an effect on the separation of metal droplets from the liquid slag. In addition to this, the slag volume also increases with an increase in basicity. Figure 4 shows the effect of the slag basicity on the V_2O_5 content

of the slag. No indication is given whether the metal particles in the slag were avoided during analysis.

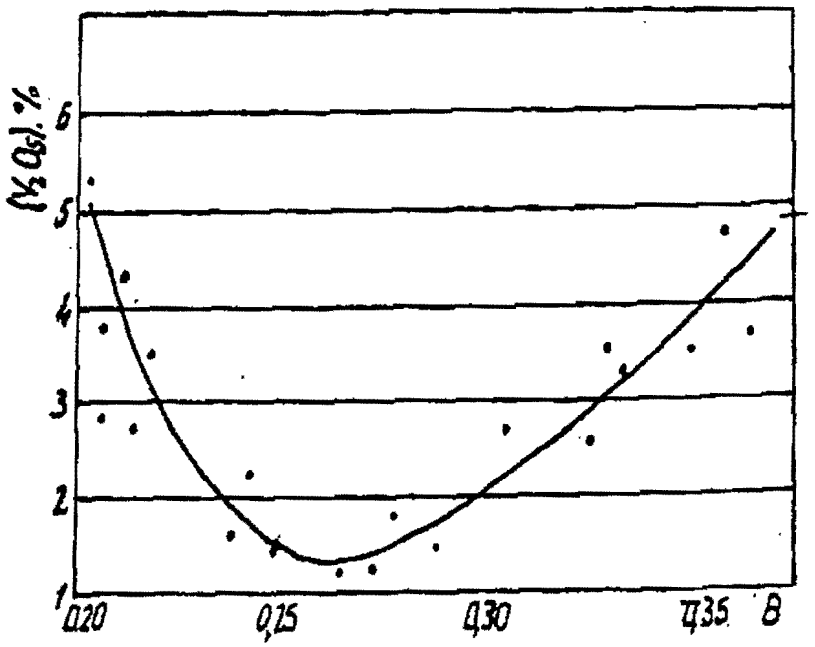

Figure 4: Effect of the slag basicity (mass %CaO / mass %Al_2O_3) on the V_2O_5 content of the slag (Nyirfa,1985).

From this figure it is evident that an optimum exists at a ratio mass % CaO: mass % Al_2O_3 of around 0.25 –0.3, which must be achieved if the recovery is to be maximized, if the effect of viscosity on the recovery can be neglected. In other words the effect of slag basicity on droplet entrainment and its subsequent contribution to the total vanadium loss to the slag are not taken into account. Nothing is mentioned about the type of refractory lining this industrial smelting process (Nyirfa,1985). As indicated later in this work a substantial amount of magnesite refractory lining dissolves in the presence of a high-alumina slag. If it is assumed that effect of MgO is similar to CaO then the effect of the former on the vanadium distribution cannot be neglected and should be incorporated in the basicity relationship. No indication is given in this work regarding the effect of slag basicity on the phenomenon of droplet entrainment.

In the next paragraph the second of the Al-based reduction processes will be discussed (i.e. electro-aluminothermic reduction).

1.2.4.3. Electro-aluminothermic production of ferrovanadium

As indicated by the title of this work, factors influencing vanadium recovery in the electro-aluminothermic process will be under detailed investigation. For a lower vanadium oxidation level in the feed material less Al is required and consequently the reaction is less exothermic. The use of V_2O_3 and V_2O_4 as raw materials necessitates the addition of external energy to sustain the reduction process. This process is much less violent and thus more controllable than the aluminothermic process. This allows the operator better control over the process because temperature is an important factor concerning the quality of the product, vanadium yield, viscosity of the slag, the separability of the slag and the metal, and the dissolution of the refractory lining. The equilibrium constant of this reduction reaction is strongly temperature dependent, thus co-determining the distribution of vanadium between the metal and the slag. Electric power consumption in ferro-alloy production is compared in Table 2. Although the production of ferrovanadium by an electric arc furnace process does not require as much power as other ferro-alloy processes, it can still amount to a substantial percentage of the total cost and should therefore be carefully controlled.

Alloy	Specification	Energy consumption (kWh/ton) of alloy
Ferrochrome	0.06 % C	18000
	1 % C	10000
	4 - 6 % C	7000
Ferrosilicon	45 % Si	6000
	75 % Si	9000
Ferromanganese	0.5 % C	7000
	1-2 % C	3000
Silico-manganese	65 % Mn	9000
Ferrotitanium	26 % Ti	7500
Ferrovanadium	80 % V	1100

Table 2: Electric power consumption in ferro-alloy production. All the electric power consumption estimates, were taken from Sieveking(1945) except that of ferrovanadium which is typical of a South African producer, with V_2O_3 as feed.

Ferrovanadium can be produced from the trivalent oxide (V_2O_3) by reduction with aluminium in an electric arc furnace, adding iron in the form of scrap, and lime (CaO) to flux the alumina (Al_2O_3) - the byproduct from the reduction reaction.

Typical compositions of the metallic product and the slag are given in Table 3, based on figures for a South African producer. A corresponding mass balance is depicted schematically in Figure 5; the mass balance shows a mismatch of some 140 kg per tonne of ferrovanadium. This is largely the result of the substantial wear of the magnesia refractory lining of the furnace for which data could be obtained; the entire MgO content of the slag (see Table 3) is the result of refractory wear in this furnace.

Table 3: Typical metal and slag compositions (mass persentages).

Metal:

V	Al	Fe	Si
80	2	17	1

Slag:

Al_2O_3	MgO	CaO	V_2O_3
65	11	21	3

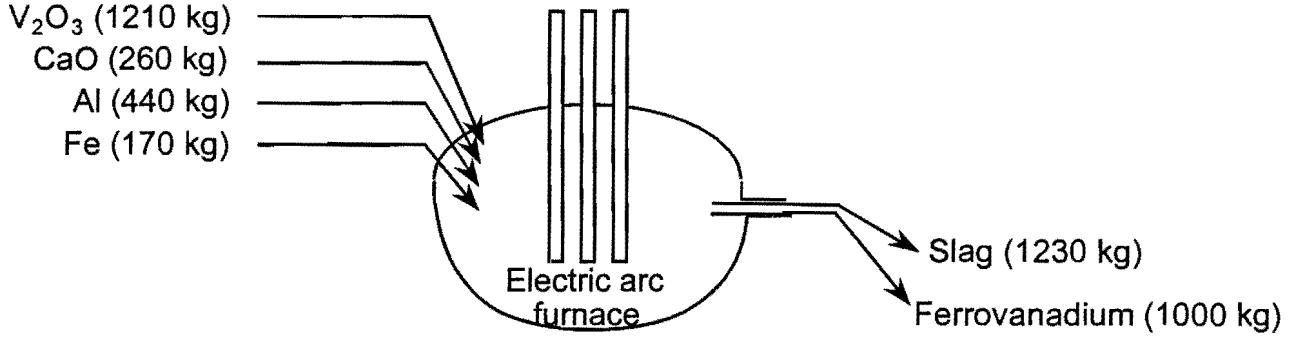

Figure 5. Schematic depiction of a ferrovanadium furnace which uses V_2O_3 as feed, with an approximate mass balance.

Excessive tap temperature can reduce the life of the magnesite refractory lining quite substantially. Recorded tap temperatures as high as 1900 °C are reported from industry. The high temperature necessitates a magnesite refractory lining, although the incompatibility between the Al_2O_3-rich slag and the lining results in excessive wear.

Point E on the line D-G in figure 6 depicts the average industrial slag composition of the South African ferrovanadium producer. If a slag, with average composition E, is brought is contact with the refractory lining, mainly MgO, the average composition of the reacting slag will change along line D-G. At a temperature of 1800°C, the slag would only be saturated with spinel ($MgO.Al_2O_3$) when the average composition reached point F, indicating that the industrial slag is not saturated with MgO.

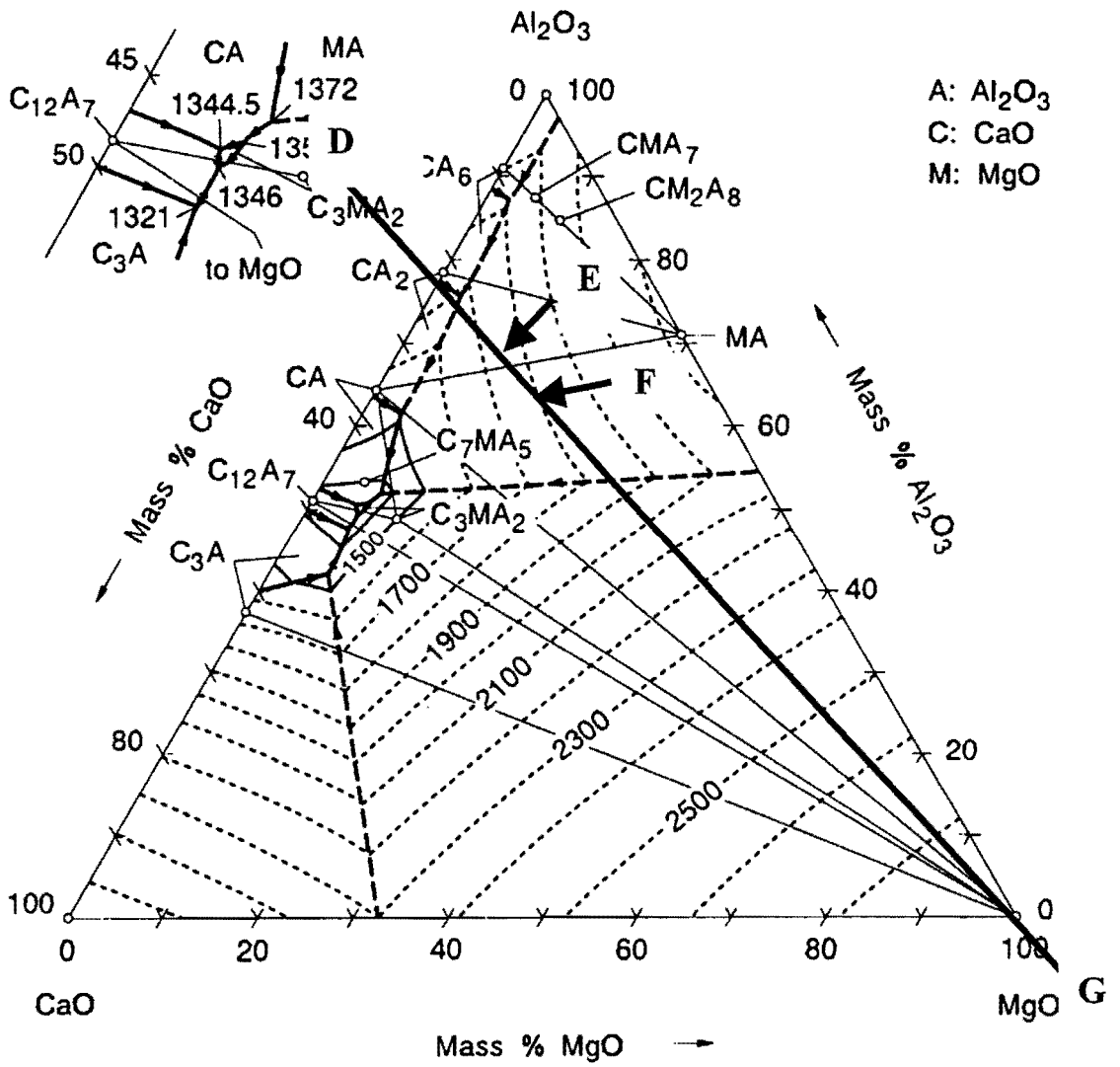

Figure 6: Al_2O_3-CaO-MgO ternary phase diagram, (Verein Deutscher Eisenhüttenleute,1995).

Industry observations indicate that deep furrows, especially around the tap hole, are observed after the completion of each heat. These deep furrows are from time to time patched up with fettling material containing around 90 % MgO. The consumption of the fettling material is on average about 70 – 100 kg per heat and this value gradually increases as more excessive wear occurs at the later stages of the lining life. This fettling practice allows the ferrovanadium producers to attain between 200 and 300 heats on a lining.

Mass balances performed and depicted in figure 5 on the smelting process showed that the high MgO content of the slag has its source from the refractory lining and the fettling

material being used to extend the life of the refractory lining. The MgO content of the slag can, thus, serve as marker of lining wear and should therefore be carefully monitored.

In addition to refractory wear due to the dissolution of the magnesite refractory lining in the Al_2O_3-rich slag, the evaporation of Mg (produced by the reduction of MgO) is possible under the prevailing conditions. The typical tap temperature is around 1800°C and an estimation of the reigning partial oxygen pressure (see section 1.5.1. on activity-composition relations) reveals values $Po_2 \approx 10^{-15}$ atmospheres. Magnesia vaporizes at low oxygen pressures and high temperatures according to the following reaction

$$MgO = Mg(g) + O_2 \qquad (6)$$

The calculated equilibrium partial magnesium vapour pressure (P_{Mg}) is 0.135 atm for a $Po_2 = 1.88 * 10^{-14}$ atm (see Table 10) at 2073K. (This was calculated using correlations of Kubaschewski et al. [1993] for free energy values.) All the fume and dust liberated during the smelting process are withdrawn from the furnace using an external suction fan. The dust is subsequently separated from the smelter exhaust gas using bag filters. The magnesium fumes emitted from the furnace re-oxidize at the colder regions higher up in the furnace during its ascent. The high MgO content of the recycled dust, shown in Table 4, is indicative of magnesium vaporisation.

Component	%
V_2O_5	54.8
CaO	2.7
Al_2O_3	32.6
MgO	8.2
Fe_2O_3	0.9
SiO_2	0.5

Table 4: Chemical composition of recycled bag filter dust of a South African ferrovanadium producer.

The flow sheet of a South African ferrovanadium producer is shown in figure 7.

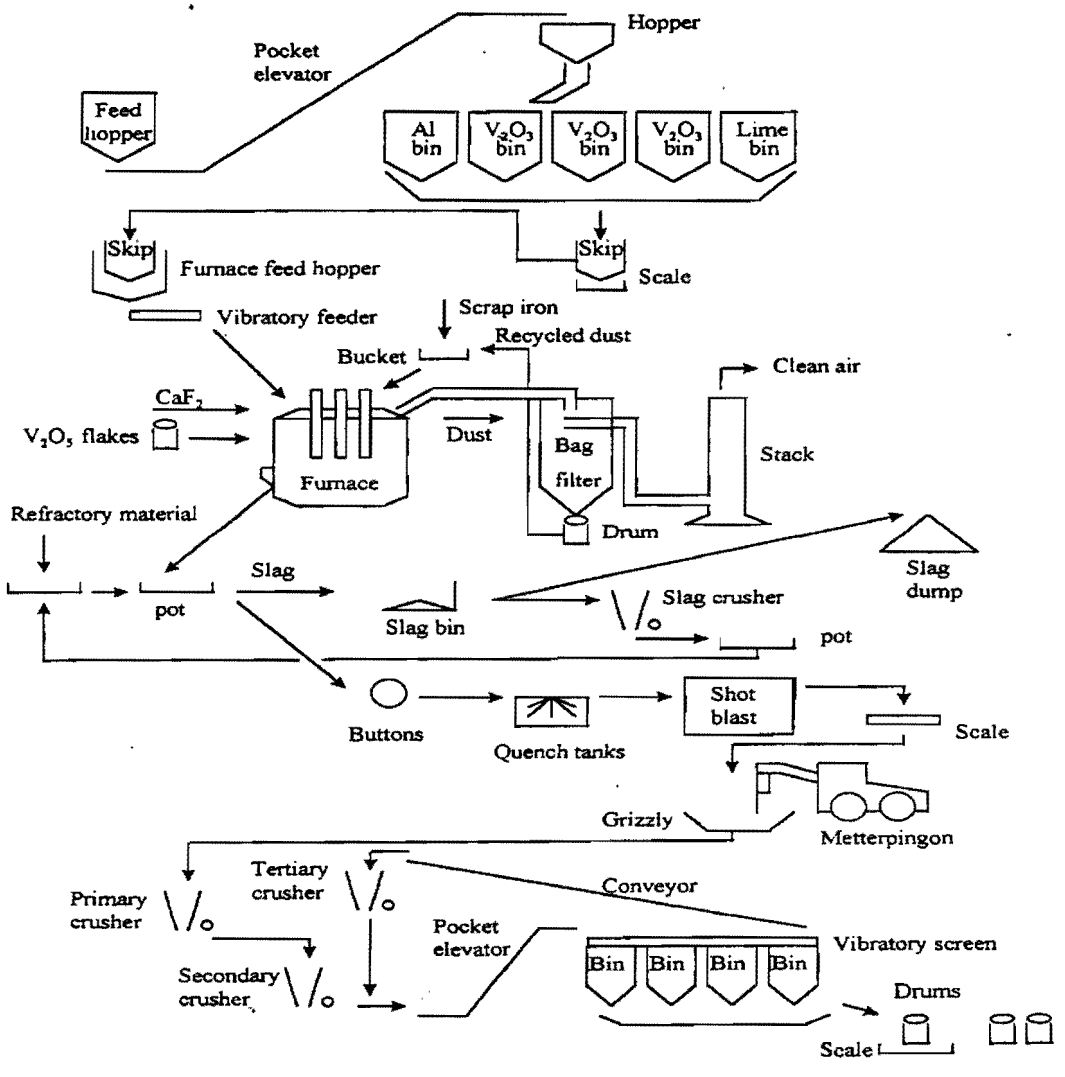

Figure 7: FeV process flow sheet of a South African producer

Fluorite is added just prior to tapping to lower the solidification temperature of the slag. The lower solidification temperature increases time available for separation of the droplets, thus increasing vanadium recovery. During the reduction process vanadium oxide is reduced to vanadium metal which subsequently reacts with molten iron and aluminium to form the metal particles. Not all metal particles, especially not the smaller ones, settle out of the slag while in the liquid state. This results in the entrainment of metal droplets. CaF_2 further enhances refractory wear leading to more vanadium oxide in the slag because MgO increases the alumina activity coefficient (See section 6.2). The time between the addition of the CaF_2 and tapping is kept as short as possible to limit the effect of the CaF_2 on the refractory lining. V_2O_5 flakes (around 230 kg for a heat size of 1100 kg FeV) are added with the raw materials to enrich the metal with vanadium.

1.2.4.4. Factors influencing vanadium recovery in the electro-aluminothermic production of ferrovanadium

The aim of this next section is to identify and evaluate all possible factors influencing vanadium recovery in the electro-aluminothermic production of ferrovanadium. The limited availability of applicable information in some instances hinders the evaluation of the process.

1.2.4.4.1. The loss of vanadium units due to theft

As in case of many valuable commodities, such as copper and nickel, a lucrative trade exists also in ferrovanadium on the black market. The price of ferrovanadium is linked mainly to the steel price and ranges from $7/kg up to $32/kg. Sporadic instances of theft are reported from time to time, but one gets the impression that this is only the tip of the iceberg. Especially the disappearance of small quantities of ferrovanadium on a daily basis will go undetected through the system. This integrated over a certain period will lead to substantial losses. A number of precautionary measures such as high fencing, security and a good and strict practice can be taken to minimize the effect of theft, although the total elimination of such trade is very unlikely. Due to the lack of information available no further discussion of theft as a possible cause of vanadium loss will be given here.

1.2.4.4.2. Loss of vanadium units as oxide spillages during handling and transportation

The fine vanadium oxide powder (consisting mainly of V_2O_3 and small quantities of VO_2) is transported by truck in metal containers (known as kibbles) from the oxide producing plant to the ferrovanadium plant. The kibbles are lifted with a fork lift onto the discharge unit located near the raw material silos. The kibble discharge hatch is subsequently opened releasing the contents into a bucket elevator unit from where the oxide is transported into the silos. An appreciable amount of oxide dust is generated during the discharge stage. The dust escapes from the bucket elevator unit through openings and is

released into the plant. In addition to the health risk posed by the dust, a substantial amount of vanadium is lost during the handling activities such as charging of the furnace. Ways have to be found to eliminate vanadium loss due to dust formation; these may include pelletizing, sintering, briquetting or the installation of a pneumatic conveying unit.

1.2.4.4.3. Loss of vanadium units as reverts

Recyclable ferrovanadium spillages which occur during the tapping process are commonly known as reverts. Some ferrovanadium smelting processes utilize a number of small tapping pots instead of one large pot. This sometimes leads to the phenomenon where metal is tapped onto solidified slag. The first few pots taking mainly the slag constituent from the furnace, are not completely filled. When on subsequent tapping the remainder of the furnace contents, now mostly ferrovanadium metal, is tapped into the remainder of the tapping pots, the capacity is sometimes exceeded. This forces the operator to re-use to the first few tapping pots, now containing solidified slag, to overcome the lack of capacity. As a result, some of the reverts are dumped together with the slag.

The reverts can be recovered by crushing and jigging of the old dump on an annual basis. Most of the misplaced ferrovanadium is now recycled as feed material to the furnace. The loss of ferrovanadium as reverts can be eliminated by utilizing a single slag pot with a capacity which exceeds that of the furnace slag content. In addition to the savings in spillage losses, a large slag pot also promotes the separation of the metal phase from the slag phase during solidification, as indicated in the next session on metal droplet separation.

1.2.4.4.4. Metal droplet entrainment

Preliminary investigations conducted on industrial slag samples show two primary mechanisms of droplet entrainment. Figure 8 and 9 show images of entrained droplets underlining the dual mechanisms leading to droplet entrainment.

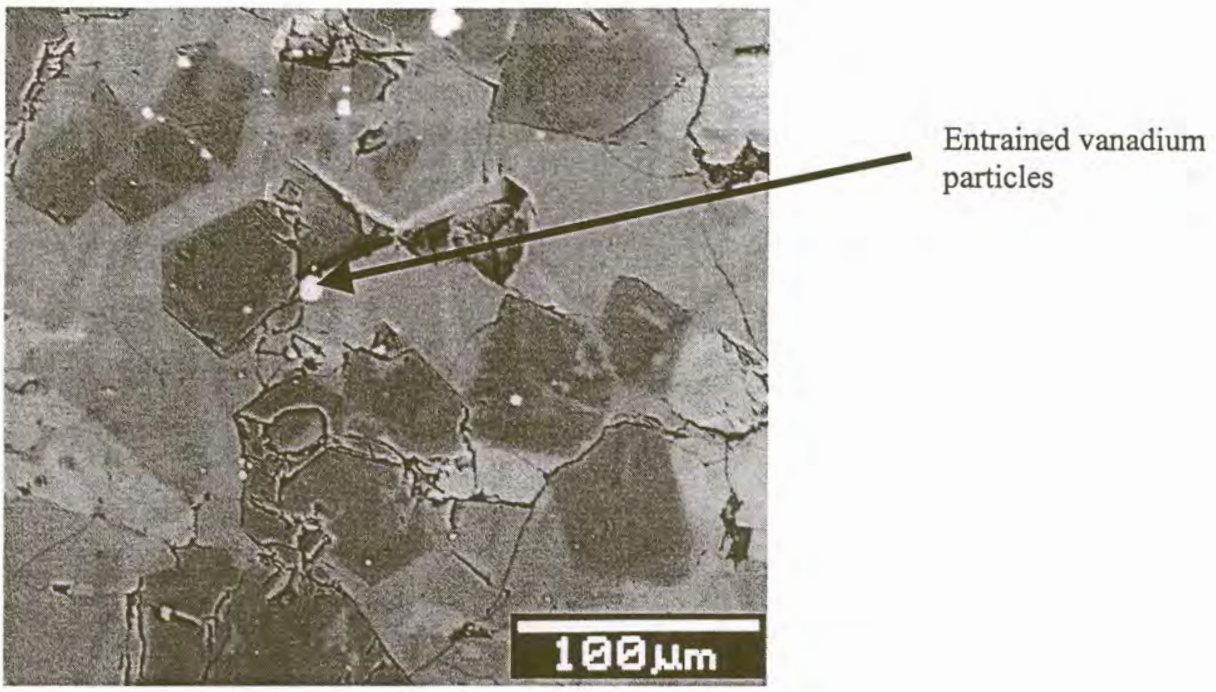

Figure 8: Back scattered electron image of vanadium droplets embedded in industrial slag sample.

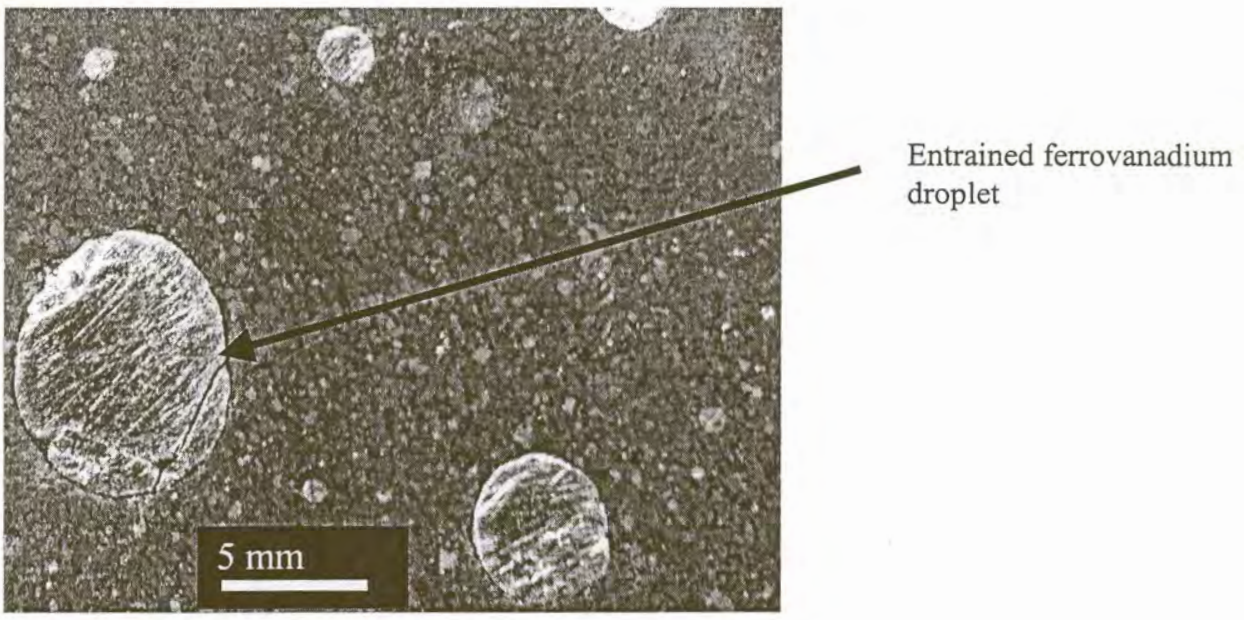

Figure 9: Entrained ferrovanadium droplets in industrial slag sample.

The results of EDS analysis conducted on the entrained droplets, depicted in figure 8 and 9, are showed in Table 5.

	V-droplets	FeV-droplets
% V	72-96	82
% Fe	0-20	15.4
% Al	0-11	1.2

Table 5: EDS-results on entrained droplets showed in figure 8 and 9

The vanadium content of the entrained droplets showed in figure 9 corresponds to the ferrovanadium bulk composition given in Table 5, indicating entrainment as a result of an incorrect tapping procedure. In other words, the entrainment can be a result of a too slow tapping stage by which ferrovanadium is tapped onto "cold" liquid slag. Not enough time is allowed before complete solidification resulting in large entrained metal droplets with a composition similar to that of the bulk metal. A re-evaluation of the tapping practice could eliminate the loss of vanadium as entrained ferrovanadium droplets.

The high vanadium content and small droplet size indicate that the droplets showed in figure 8 are most probably as formed during the reduction process before alloying with iron. Pure vanadium droplets are formed when the vanadium containing oxides are initially reduced by molten aluminium. The metallic droplets now agglomerate and separate from the slag phase under their combined weight. The pure vanadium droplets subsequently form an alloy with the molten scrap iron in the bottom of the furnace. The generally low iron content of the vanadium droplets indicates the lack of intimate contact between the droplets and the molten iron pool. The vanadium recovery will increase with the utilization of larger tapping pots due to the decrease in the cooling rate and the subsequent increase in the metal separation periods, thus, yielding higher metal recoveries. The influence of slag properties on the separation of the solid phase will be discussed in the section on the influence of physicochemical properties of the slag on the separation of the solid phase

1.2.4.4.4.1. Influence of physicochemical properties of the slag on the separation of the solid phase.

Any liquid-solid separation process can be divided into either free or hindered settling conditions. The crowding of particles is negligible in free settling conditions, whilst particle crowding becomes more apparent in hindered-settling conditions. Effectively all the resistance to motion in viscous slag systems is due to the shear forces or viscosity of the fluid. In addition to this, preliminary results show the average entrained droplet diameter to be 0.5 μm for V-particles and 5 mm for FeV-particles. The separation of metal particles or droplets from the slag therefore obeys Stokes' law, which assumes the drag force of spherical particles to be entirely due to viscous resistance, giving the expression.(Wills,1993)

$$D = 3\pi d\eta v \qquad (7)$$

With d = spherical particle diameter(m)
D = drag force (N)
η = slag viscosity (Pa.s)
v = terminal velocity (m/s)

and

$$v = gd^2(\rho_s - \rho_f)/18\eta \qquad (8)$$

with ρ_s = particle density (kg/m^3)
ρ_f = slag density(kg/m^3)

$\rho_s - \rho_f$ is know as the effective density of the particle and is fairly constant when slag and ferrovanadium with constant composition are produced.

Thus, the viscosity of the slag has a large effect on the settling rate of solid particles. The viscosity of the slag is mainly influenced by temperature, slag composition and the presence of solid particles. The relative viscous resistance on small spherical particles is

much larger than on large spherical particles with the same effective density. If the entrained particles are large enough to benefit from a lower slag viscosity, a rise in the tap temperature will reduce droplet entrainment. The beneficial effect of temperature on droplet entrainment may unfortunately be counterbalanced by the increase of soluble vanadium in the slag. The effect of slag composition on the viscosity of the slag will now be addressed.

Al_2O_3-rich Al_2O_3-CaO slags are formed during the manufacture of ferrovanadium. The dissolution of the magnesite refractory lining in the acidic slag has a fluxing effect on the slag. Figure 10 shows the Al_2O_3-CaO-MgO ternary phase diagram. (Verein Deutscher Eisenhüttenleute,1995)

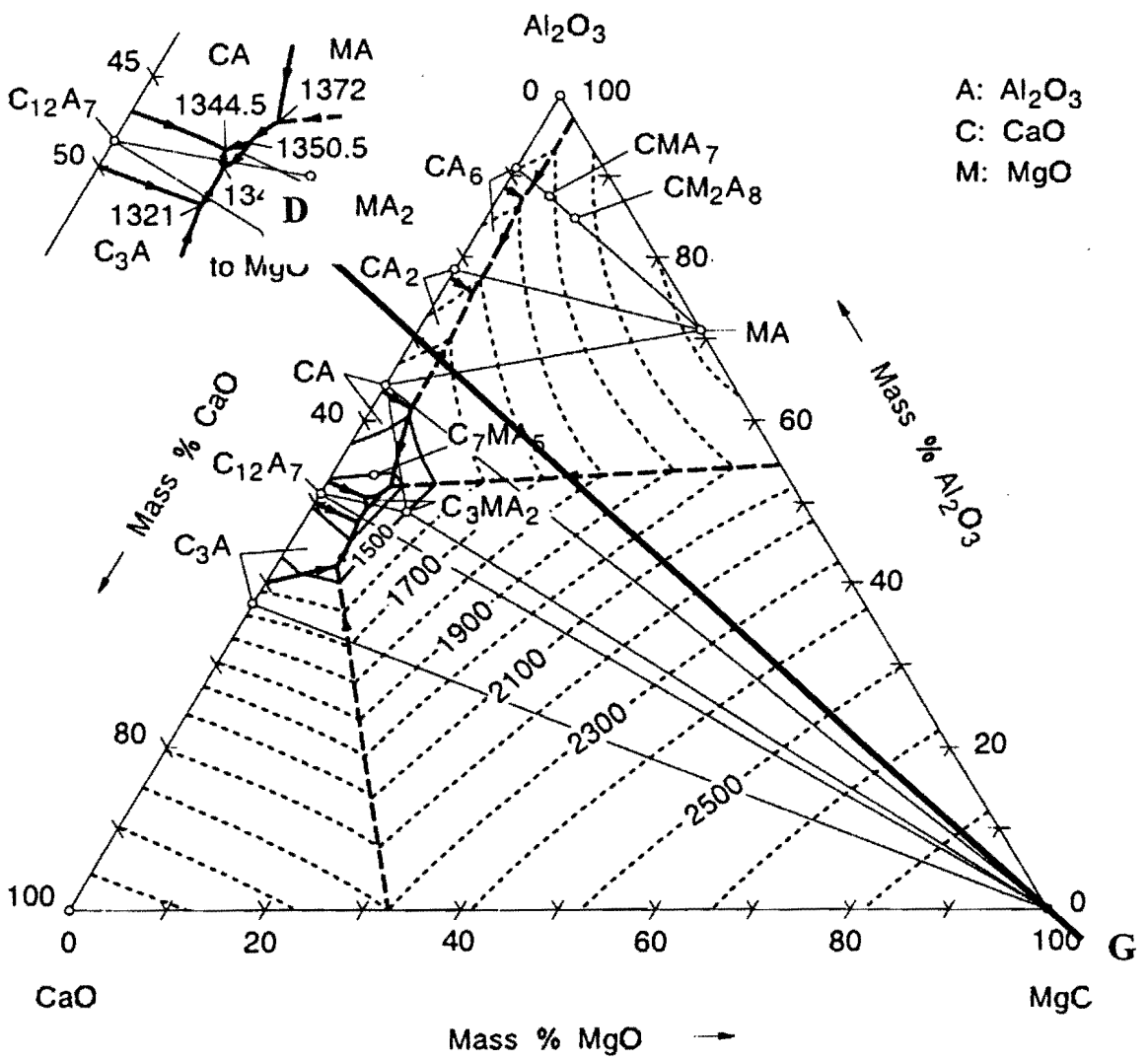

Figure 10: Al_2O_3-CaO-MgO ternary phase diagram (Verein Deutscher Eisenhüttenleute,1995).

If, for example, 70 % Al_2O_3- 30 % CaO slag is brought into contact with MgO from the lining the nominal composition will change alongside the line D-G. A small quantity of MgO (~4 %) will reduce the melting point of the slag from 1650 °C (the melting point of a 70 % Al_2O_3-CaO slag) to ~1580 °C. At the industry-reported maximum of around 10 % MgO, the liquidus temperature again reaches 1650°C. Upon further dissolution of MgO the melting point will increase and presumably so too the viscosity of the slag (at a given temperature).

The longer the slag is in the liquid state and the lower its viscosity when molten the more complete will be the separation of metal and slag. The effect of CaO and MgO fluxing additions on the viscosity of high-alumina slags can be seen in figure 11 (Arkhipov,1965). Their study focused on factors effecting the more complete separation of the metal and slag phases. Physicochemical properties such as slag viscosity, composition, surface tension, interfacial tension and liquidus range of around 100 laboratory heats were studied. Three distinct slags were used to illustrate the influence of fluxing additions on the metal droplet separability. The composition of the three slags used is shown in Table 6.

	SiO_2	Al_2O_3	CaO	TiO_2	MgO
Slag 1	0.07	86.9	2.2	0.35	1.41
Slag 2	0.11	84.5	6.6	0.37	0.98
Slag 3	0.22	80.2	6.4	0.32	4.73

Table 6: Composition (mass percentages) of the three slags used to illustrate the effect of fluxing additions on droplet entrainment(Arkhipov,1965). Despite the chemical compositions not adding up to 100%, it can still be assumed that three slags with distinct alumina contents were employed.

Nothing is mentioned about the nature of the laboratory experiments conducted to give rise to the results shown in figure 11. A nominal vanadium content of 85 % in the ferrovanadium was aimed for. Figure 11 depicts the results as obtained from the three slag samples.

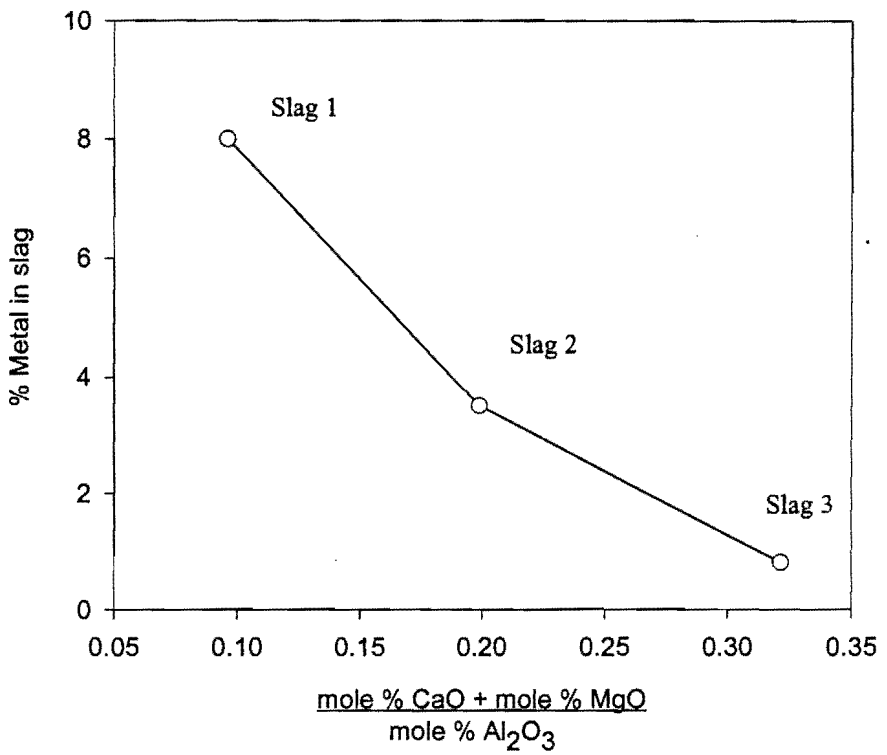

Figure 11: Metal droplet entrainment (expressed as percentage metal in the slag) as a function of slag basicity (after Arkhipov, 1965).

The Al_2O_3 content of the slag of the South African ferrovanadium producer is considerably lower, see Table 3, than the tabulated values reported by the authors. The results depicted in figure 11, show that a slight alteration in the chemical composition of the slag formed in the aluminothermic production of ferrovanadium has a considerable effect on the separation of the liquid phases, at low basicity.

In order to attain a better understanding in the causes behind the more complete separation of the liquid phases, viscosity measurements can be carried out on synthetic slags. Viscosity investigations were carried out by Arkhipov et al (1965) on slags produced in the production of ferrovanadium. Table 6 show the composition of the high-alumina slags used in these investigations. The viscosity measurements were carried out in a vertical resistance tube furnace using a carbon reduction tube in which temperatures around 2100°C were reported. The temperature within the furnace was measured by

means of a tungsten-molybdenum thermocouple, and the viscosity of the slag was determined by means of a vibration viscosimeter. The influence of the fluxing additions CaO and MgO on the viscosity on high-alumina slags is depicted in figure 12.

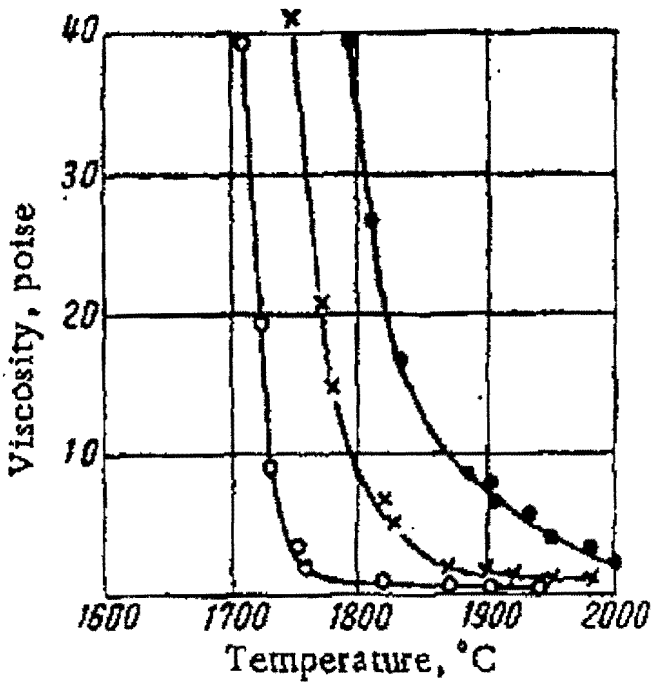

Figure 12: Viscosity curves of high-alumina slags (• Slag1, × Slag2, o Slag3) (Arkhipov,1965)

It is evident from the curve that slag 3 provides the best conditions of droplet separation in the temperature range of 1750 °C – 2000 °C. Slags which give optimum vanadium recovery must have a minimum viscosity prior to solidification as well as an optimum composition to ensure minimum soluble vanadium loss. The term soluble vanadium loss refers to oxidic vanadium in the slag. If, for example, the alteration of the slag composition by adding fluxing agents, is not beneficial to vanadium recovery with respect to soluble vanadium loss, then the separation of the liquid phases can be optimized by tapping at a slightly higher temperature and utilizing a larger melt volume. The smaller the volume of the melt the more rapid the heat transfer to the surrounding environments. Figure 13 shows cooling curves of a range of slag compositions as well as that of an alloy containing 85 % vanadium and 8.2% iron. The composition of each slag used is given in

Table 6 and the cooling curve of each slag is numbered accordingly. Cooling curve four refers to the cooling curve of the alloy.

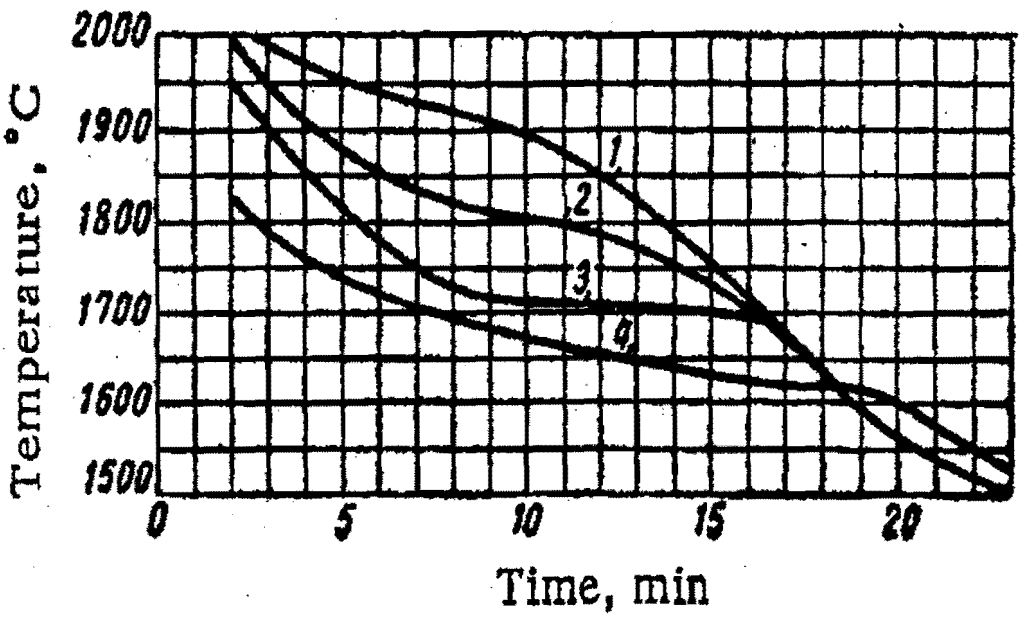

Figure 13: Cooling curves of slags after termination of smelting process (Arkhipov,1965). 1) Slag 1; 2) Slag 2; 3) Slag3; 4)Alloy, containing 85% vanadium and 8.2% iron.

Figure 11 shows that slag 3 has the lowest melting point and it remains in the liquid state longer thus representing the most favorable conditions for separation.

In addition to slag composition and temperature, solid particles in the slag also have an influence on the viscosity of liquid slag. The effect of solid particles on the viscosity behavior of slag was studied by Reddy et al (1993). The existence of solid particles result in significant increase in the slag viscosity as shown in figure 14.

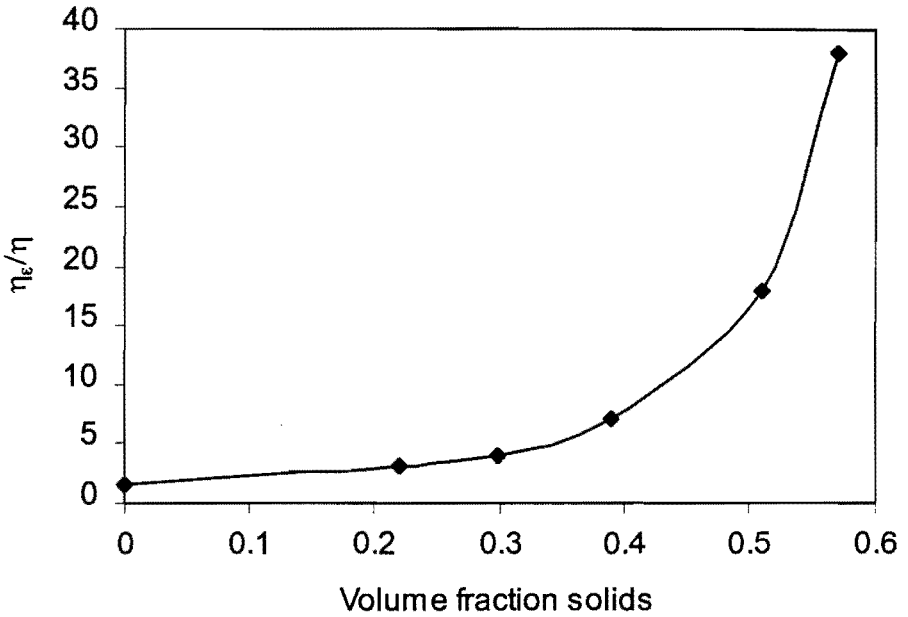

Figure 14: Influence of the solid content of the melt on the ratio of apparent viscosity to that of the pure liquid.(Reddy,1993)

When the volume fraction of solid particles increases to 0.57 the effective viscosity increases almost to 38 times the viscosity of the pure liquid. The melting point of the ferrovanadium droplets is higher than the liquidus temperature of the slag (See figure 17 for a 80 % V alloy. The binary Fe-Al and Al-V phase diagrams [Baker,1992] show the small effect of small amounts of aluminium on the melting points of these alloys. It may be assumed that small amounts of Al have a similar effect on the melting point of ferrovanadium), resulting in the formation of solid particles while the slag is still in the liquid state. It is debatable whether the entrained droplets in the ferrovanadium slag will have this appreciable effect on the viscosity due to the comparatively low concentration of droplets in the slag. Arkhipov and co-workers (1965) reported values between 0.8 and 8 % of metal produced end up in the slag. (This works out to be around 3 volume % particles in the slag, assuming 1000 kg metal and 1400 kg slag produced, with the slag containing 8 % of total mass of alloy produced. Metal and slag densities were taken to be 5800 kg/m^3 and 2600 kg/m^3 respectively.)

With regard to the viscosity, the slag with the lowest melting point and the fewest droplets should be used to maximize metal droplet separation. This does not, of course, mean that vanadium recovery in total will also benefit because the effects of viscosity, temperature

and slag basicity in vanadium recovery are interwoven. The aim of this study is to address this issue in order to optimize vanadium recovery.

1.2.4.4.5. Vanadium loss due to unreduced oxides in the high alumina slag

One way to decrease the amount of unreduced oxides in the slag is to add excess aluminium as reducing agent to the feed material. A certain amount of aluminium reductant ends up in the product as an impurity since aluminium readily alloys with many metals and alloys. In addition to aluminium loss to side reactions and atmospheric oxidation, some aluminium is vaporized at the tip of the electrodes.

International consumer specification on the residual aluminium content of ferrovanadium limits the use of too much excess aluminium. Optimum vanadium content of the slag should be aimed for while still meeting international consumer specifications. One way to accomplish high vanadium yields without adding too much excess aluminium is to manipulate factors influencing the vanadium activity coefficient in the slag. The overall oxidation reaction can be expressed as

$$2(V)_{FeV} + (Al_2O_3)_{slag} = 2(Al)_{FeV} + (V_2O_3)_{slag} \qquad (9)$$

The experimental work(reported later in this thesis) determined the oxidation state of oxidic vanadium, but for illustrative purposes the oxidation state vanadium is here taken as V^{3+}. The equilibrium activity of vanadium oxide in the slag is given by

$$a_{V_2O_3} = K\frac{a_V^{\,2}\, a_{Al_2O_3}}{a_{Al}^{\,2}} \qquad (10)$$

with

a_x = activity of species x

K = equilibrium constant

The activity coefficient of vanadium oxide is likely to be strongly influenced by the slag basicity, thus strongly influencing the vanadium distribution between the metal and the slag. By optimizing the activity coefficient through the careful adjustment of the slag basicity the tendency of oxide formation can be greatly reduced. The effect of slag basicity on the vanadium content of the slag is depicted in figure 4. The same strong effect is also expected to hold for the electro-aluminothermic reduction.

In practice the adjustment of the slag basicity by adding large quantities of fluxing agents is limited by the furnace dimensions, power rating and whether the large slag volumes will prevent the electrodes from arcing. Nevertheless, a strong vanadium-content composition relation as depicted in figure 4 indicates that only small adjustments in slag composition are necessary to increase recoveries.

1.3. Thermodynamic properties

1.3.1. Systems similar to vanadium system

There is not much literature available on the influence of slag basicity on the vanadium oxide activity in the Al_2O_3-CaO-MgO systems. It is known that species with the same ionic radii and oxidation state will behave similarly in liquid slags. Table 7 below shows corresponding ionic radii for the same oxidation state of a few different species.

Species	Ionic radius (nm)	Species	Ionic radius (nm)	Species	Ionic radius (nm)
V^{2+}	0,88	Ti^{2+}	0,94	Cr^{2+}	0,89
V^{3+}	0,74	Ti^{3+}	0,76	Cr^{3+}	0,63
V^{4+}	0,63	Ti^{4+}	0,68	Cr^{6+}	0,52
V^{5+}	0,59				

Table 7: Ionic radii of a few oxidized species.(Weast,1982)

It is evident that V^{2+} and Cr^{2+}, Ti^{3+} and V^{3+} are expected to behave similarly in liquid slag systems. Figure 15 below shows the effect of slag basicity on the partitioning of chromium between the Cr^{2+} and Cr^{3+} oxidation states.

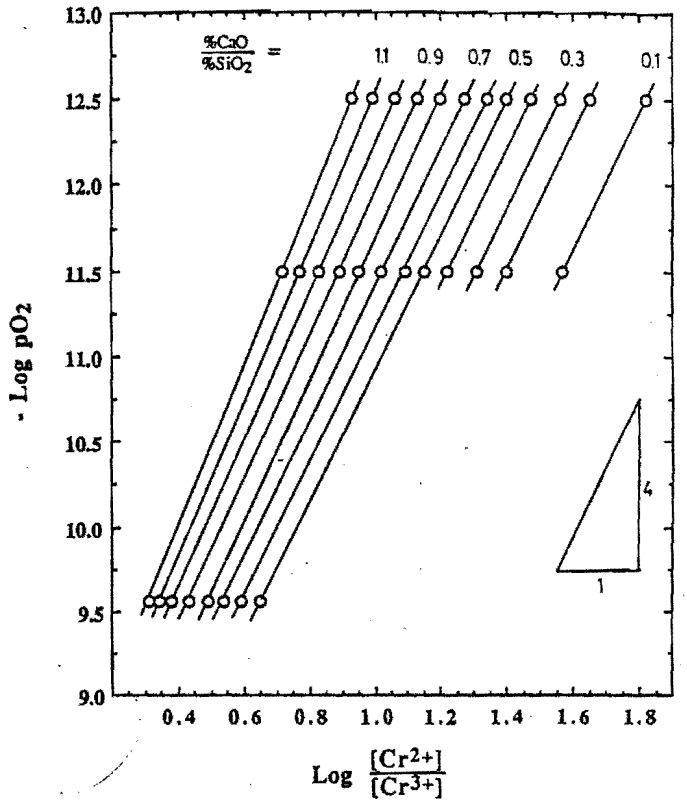

Figure 15: Effect of slag basicity on the partitioning of chromium between the oxidation states (Pretorius,1989).

The figure indicates Cr^{2+} to be more stable at low oxygen partial pressures and low basicities. According to this V^{2+} is expected to be the prominent oxidation state where conditions of low oxygen pressure and low basicities prevail in silica melts. The interactions between species in liquid melts are usually non-ideal and highly species dependent. Because of this it cannot be said that V^{2+} will be the more stable oxidation state in Al_2O_3-CaO melts where conditions of low partial oxygen pressure and low basicities prevail.

1.3.2. Estimation of the reigning partial oxygen pressures in the industrial FeV-production process.

The oxidation equilibrium of vanadium at fixed partial pressures in the industrial FeV-production process can be either reaction (13) or (14)

$$V + 0.5O_2 \rightarrow VO \quad (13)$$

$$2V + 1.5O_2 \rightarrow VO_{1.5} \quad (14)$$

The oxygen partial pressure in industrial smelting processes is governed by those reactions which remain closest to equilibrium. In the vanadium smelting process where Al is used as a reductant the Po_2 partial pressure is most probably governed by reaction (15)

$$2Al + 1.5O_2 \rightarrow Al_2O_3 \quad (15)$$

The overall reactions can thus be expressed as

$$V + Al_2O_3 \rightarrow Al + VO \quad (16)$$

$$V + Al_2O_3 \rightarrow Al + V_2O_3 \quad (17)$$

The reigning partial oxygen pressure in the vanadium smelting process can be calculated as follows

$$P_{O_2} = \left(\frac{a_{Al_2O_3}}{a^2_{Al}\, e^{-\frac{\Delta G^0}{RT}}} \right)^{\frac{2}{3}} \quad (18)$$

The assumption is that reaction 15 is at equilibrium. As indicated by equation 18, the Al_2O_3 and Al activities govern the oxygen partial pressure. Figure 16 shows the activity of Al_2O_3 in binary $CaO\text{-}Al_2O_3$ slags a function of slag composition and temperature.

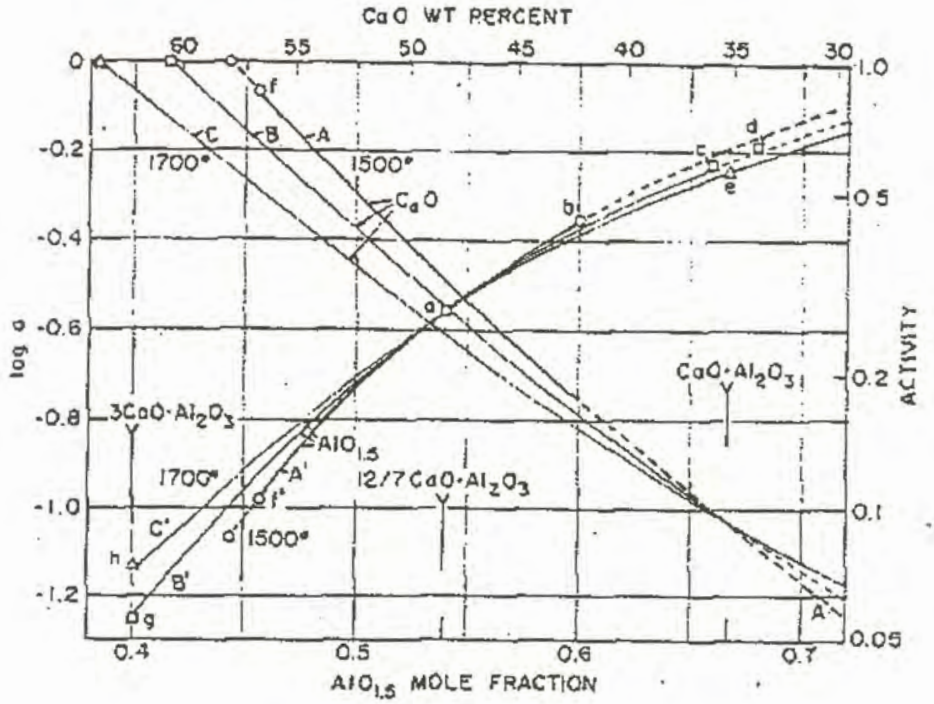

Figure 16: Al_2O_3-activity as a function of temperature and slag composition.(Rein & Chipman,1965).

Unfortunately Al_2O_3 – activity values are given in figure 16 only for melts containing a minimum of 30 % CaO (industrial slags contain 23 % CaO and 9 % MgO). The activity of Al_2O_3 in 30 % CaO-Al_2O_3 melts was hence be used for further calculations in this section.

All forms of vanadium dissolve completely and evenly in liquid steel and do not give rise to segregation nor do they form gross inclusions. The complete liquid and solid (at high temperature) solubility of vanadium and iron is depicted by the vanadium-iron phase diagram in figure 17.

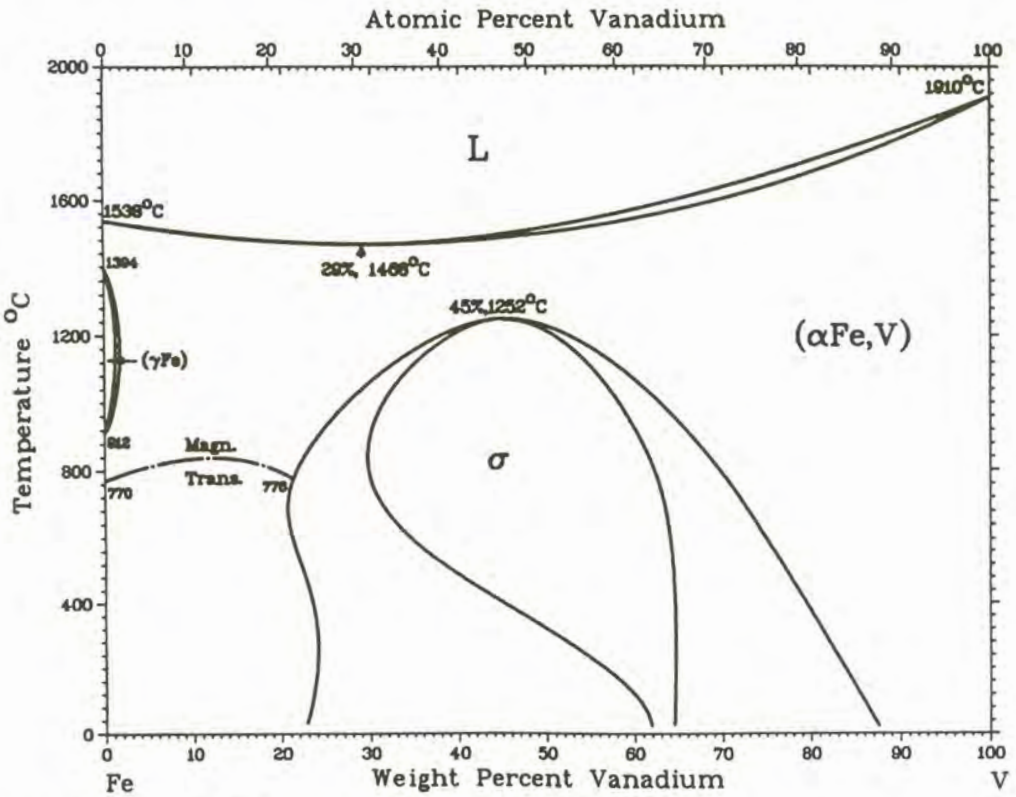

Figure 17: Binary V-Fe phase diagram. (Baker(ed))

The activity coefficient of dilute aluminium in ferrovanadium can be estimated by assuming it to be similar to that in binary Fe-Al alloys (because of the nearly ideal behavior between iron and vanadium).

Consider the following reaction for liquid iron

$$Al(l) \rightarrow Al\,(l)_{1\%} \tag{19}$$

According to Sigworth & Elliott (1974) the free energy change can be calculated

$$\Delta Gs = RT \ln\left(\gamma^{\infty}_{Al}\frac{0.5585}{M_i}\right) \tag{20}$$

With Fe as solvent and M_i = molar mass of aluminium, and γ^{∞}_{Al} the Raoultian activity coefficient for Al in a highly dilute solution. ΔGs for reaction (14) expressed as a function of temperature is as follows (Sigworth & Elliott,1974)

$$\Delta Gs = (-3609 - 1.594T) * (4.184)^2 \text{ (J/g-atom)} \tag{21}$$

The Henrian activity is simply proportional to the Raultian activity as follows

$$a_i = h_i C_i \tag{22}$$

Where the value of C_{Al} for Aluminium dissolved in liquid iron is given by:

$$C_{Al} = \frac{M_{Al}}{0.5585\gamma^{\infty}_{Al}} \tag{23}$$

and

$$h_{Al} = f_{Al}(\%\ Al) \tag{24}$$

$$\text{with } \log f_{Al} = \sum e^{j}_{Al}(\%j) + \sum r^{j}_{Al}(\%j)^2 \tag{25}$$

Where e^{j}_{Al} and r^{j}_{Al} are the first and second order interaction coefficients of species j with Al.

The following average metal composition is assumed for the sake of the calculation.

	Mass %	N_i(mole fraction)
C	0,6	0,02
Al	2	0,04
Si	0,8	0,14
Fe	14,2	0,126
V	82,4	0,8

Table 8: Average metal analysis.

The activity of Al in FeV as estimated using the metal composition given in Table 8 is shown in Table 9.

Temp(K)	Gamma Al	Ci	f_0	a_{Al}
1873	0.0291	0.0006	1.3908	0.0017
1898	0.0307	0.0006	1.3908	0.0018
1923	0.0324	0.0007	1.3908	0.0019
1948	0.0340	0.0007	1.3908	0.0020
1973	0.0358	0.0007	1.3908	0.0021
1998	0.0375	0.0008	1.3908	0.0022
2023	0.0393	0.0008	1.3908	0.0023
2048	0.0412	0.0009	1.3908	0.0024
2073	0.0431	0.0009	1.3908	0.0025
2098	0.0450	0.0009	1.3908	0.0026
2123	0.0470	0.0010	1.3908	0.0027
2148	0.0490	0.0010	1.3908	0.0028
2173	0.0510	0.0011	1.3908	0.0029
2198	0.0531	0.0011	1.3908	0.0031
2223	0.0552	0.0011	1.3908	0.0032
2248	0.0573	0.0012	1.3908	0.0033
2273	0.0595	0.0012	1.3908	0.0034

Table 9: Estimated Al-activity as function of temperature for FeV containing 2 mass % Al.

The calculated partial oxygen pressures, assumed to be fixed by Al/Al_2O_3 and $VO/VO_{1.5}$-equilibrium, are given in Figure 8.

These were calculated using correlations of Kubaschewski et al. (1993) for free energy values.

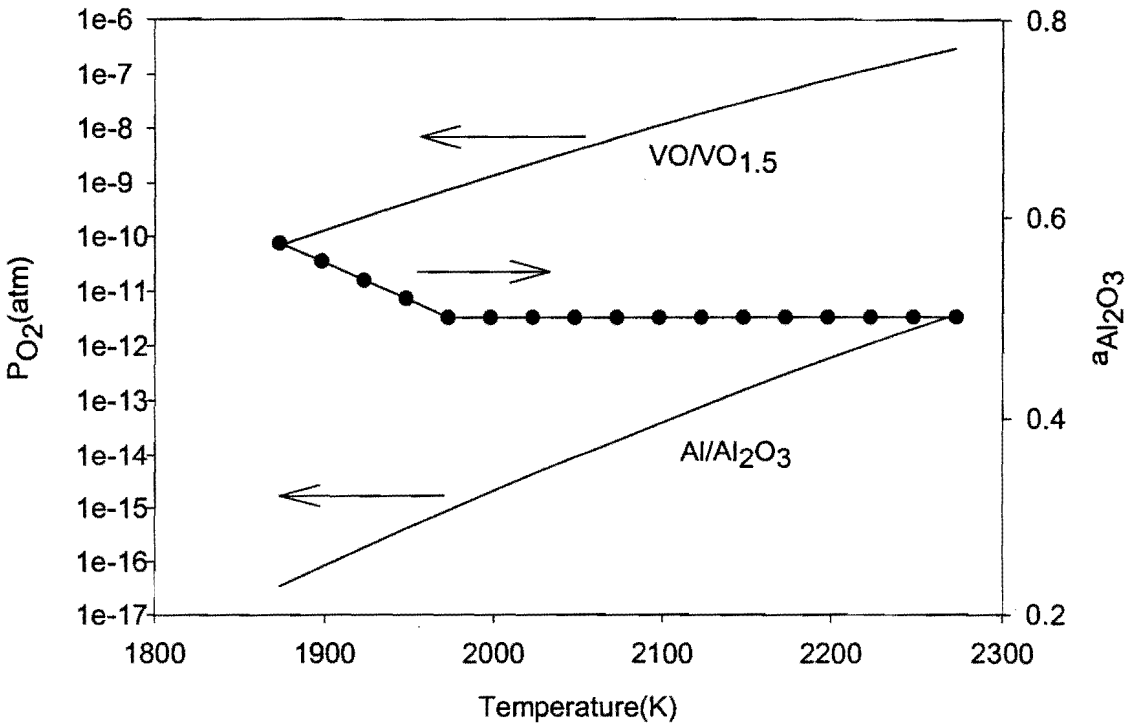

Figure 18: Comparative oxygen activities as function of temperature for the Al/Al_2O_3 and $VO/VO_{1.5}$- equilibrium. The dotted line gives the data on the activity of Al_2O_3 in 30 % $CaO\text{-}Al_2O_3$ slags. Unfortunately the literature data are given only for the 1600-1650 °C temperature range. The activity of Al_2O_3 above this range was assumed to be constant due to the lack of more accurate relations. Unit activities of VO and $VO_{1.5}$ were assumed.

Figure 18 depicts the calculated oxygen activity for the two different equilibria in the industrial ferrovanadium reduction process. This figure further indicates that V^{2+} will be the stable oxidation state if the oxygen activity is governed by the Al/Al_2O_3-equilibrium and $\gamma_{VO} \approx \gamma_{VO1.5}$. The oxidation state of vanadium in the slag clearly needs to be clarified by performing high-temperature equilibrium experiments.

These approximate oxygen activities serve to indicate the range of the oxygen activities to be used for experimental purposes in order to simulate conditions in the industrial smelting process.

1.4. Research problem and objectives

During the submerged-arc smelting process, vanadium oxide is reduced with aluminum to form ferrovanadium and Al_2O_3-CaO-MgO-slag. In addition to vanadium lost as unreduced oxides in the slag, vanadium yield is also decreased by entrained droplets, which remain in the slag after solidification. The high-alumina slag is fluxed with CaO and MgO. The entire MgO content of the slag is the result of refractory wear. A strong effect on vanadium activity of the Al_2O_3 content of the slag is expected. Adding fluxing agents in moderate quantities should minimize the detrimental effect of droplet entrainment. The South African ferrovanadium producers operate the smelting process at considerably lower Al_2O_3-values compared to aluminothermic processes, which is not necessary beneficial to vanadium recovery. The aim of this work is to quantify the effect of slag composition on the equilibrium vanadium oxide content, and on the entrainment of droplets in the slag. Knowing these relations, certain adjustments can be made to optimize vanadium recovery in the electro-aluminothermic process.

The experimental work aimed to determine the following:

- To determine the activity coefficient of VO_x as a function of the slag composition. The experiments involve fixing the oxygen activity, to a level which corresponds to the oxygen activity in the industrial smelting process, by using an appropriate gas mixture

- To determine the activity coefficient of VO_x as a function of temperature.

- To determine the oxidation state of vanadium in the slag.

- To quantify the losses of vanadium as entrained droplets as a function of slag composition.

- To quantify the total vanadium loss as a function of slag composition.

The aim of the next section is to survey different experimental techniques and procedures necessary to generate the appropriate results.

1.5. Investigation into experimental techniques and procedures

1.5.1. Evaluation of different gas mixing systems

The most versatile method used to obtain desired oxygen fugacities at high temperature is the use of two gases, which react with each other at high temperatures to release or consume oxygen. This buffering action serves to maintain the oxygen activity at a constant value.

In other words equilibrium is restored by the dissociation of the gas phase by the following reactions (as examples).

$$2H_2O = 2H_2 + O_2 \quad (26)$$

$$2CO_2 = 2CO + O_2 \quad (27)$$

In these two-gas systems the oxygen pressures are a function of temperature as well as the gas composition. The two most widely used two-gas systems are the CO_2-CO and the CO_2-H_2 systems. The complexity of the gas systems is reduced because the gas species are bought in separate cylinders ready for mixing to their specified volumetric proportions. However, at high experimental temperatures and low partial oxygen pressures, C tends to precipitate according to the following reactions.

$$2CO(g) = CO_2(g) + C(s) \quad (28)$$

or

$$CO_2 = C + O_2 \quad (29)$$

The applicability of the CO/CO_2 gas mixtures at low partial oxygen pressures is therefore limited. Working at very low oxygen partial pressures, and high temperature also limits the use of the H_2-CO_2 system because very low CO_2 flow rates are required. (for example: Volume % $CO_2 \approx 0{,}01$ at 2000 °C and $Po_2 = 1*10^{-14}$ atmosphere (Janaf table,1965).

Rotameters to control the exact volumetric flow rates of the gas species are not sensitive enough for such low flow rates, thus limiting the application range of the H_2/CO_2 gas mixtures as well.

Since oxygen partial pressures, in the range of 10^{-12}-10^{-17}, require CO/CO_2 and H_2/CO_2 ratios outside the limits of the gas mixing system, one should revert to H_2/H_2O gas mixtures as last alternative.

Table 10 gives the required water vapor partial pressure in hydrogen if the oxygen fugacity in the industrial smelting process is governed by the Al/Al_2O_3-reaction. According to Belton (1998) the lowest water/hydrogen ratio which have been used successfully was 0.002. The problem with lower ratios is that the equilibrium can only be approached practically from one direction because of the low oxygen capacity of the gas mixture. One should keep in mind that the approximations of the oxygen activity governed by the Al/Al_2O_3-equilibrium is based on the assumption that Al in ferrovanadium behaves like aluminium in dilute iron alloys. Performing an equilibrium run at the ultra-low water/hydrogen ratios at a corresponding industrial slag basicity, to see if the same vanadium content can be obtained can test the validity of this assumption. If not, the water/hydrogen ratio can be adjusted accordingly.

Although very low oxygen partial pressures can be attained certain complexities are introduced, specially referring to the gas mixing apparatus. With H_2-H_20 mixtures, hydrogen is saturated with water vapour by passing it through distilled H_20 or any other liquid substance with a well-known water partial pressure (as function of temperature). The vapour pressure of the water is only temperature dependent while the total gas flow is also pressure (total pressure above solution surface) dependent, resulting in a complex system. The gas mixing apparatus will be discussed in more detail in the next section.

Temp	ΔG°_{rxn}	Po_2	PH_2/PH_2O	PH_2O
1873	285811.8	3.36E-17	17827.2	5.609E-05
1898	282902.0	7.91E-17	14386.5	6.950E-05
1923	279990.7	1.82E-16	11684.6	8.558E-05
1948	277077.9	4.08E-16	9548.4	1.047E-04
1973	274163.9	8.94E-16	7850.1	1.274E-04
1998	271248.7	1.97E-15	6410.0	1.560E-04
2023	268332.4	4.26E-15	5261.1	1.900E-04
2048	265415.1	9.02E-15	4339.6	2.304E-04
2073	262496.9	1.88E-14	3596.6	2.780E-04
2098	259577.9	3.84E-14	2994.5	3.338E-04
2123	256658.1	7.72E-14	2504.3	3.992E-04
2148	253737.7	1.53E-13	2103.3	4.752E-04
2173	250816.8	2.97E-13	1773.9	5.634E-04
2198	247895.3	5.69E-13	1501.9	6.654E-04
2223	244973.5	1.08E-12	1276.6	7.827E-04
2248	242051.3	2E-12	1089.1	9.173E-04
2273	239128.9	3.67E-12	932.5	1.071E-03

Table 10: Required partial water pressure as a function of temperature, for Po_2 governed by the Al/Al_2O_3-reaction .

1.5.2. Experimental evaporation technique and procedure

Evaporation techniques involve a pure gas being passed over or through a liquid to produce a mixture between the gas and vapour from the liquid.

Gas entering the dispersion bottles shown in figure 19 is dispersed into bubbles, which rise in close contact with the liquid to the surface.

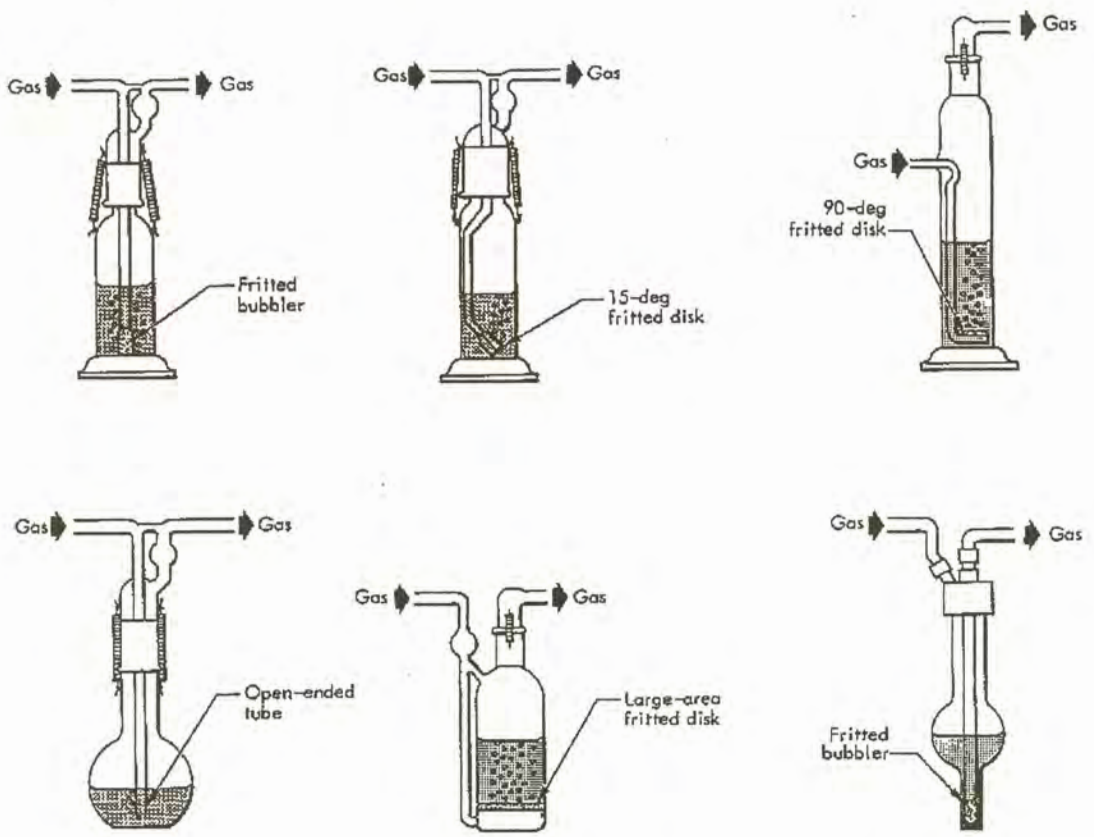

Figure 19: Sketches of six typical gas dispersion bottles.(Nelson,1992)

The smaller the bubbles the larger the cumulative surface area, and the better the efficiency of evaporation. The degree of evaporation is a function of the bubble size, rate of ascent, temperature of liquid, the retention time, total pressure on system, vapour pressure and viscosity.

Checks on the exit gas composition are absolutely essential due to the complexities being introduced by the H_2O-H_2 mixtures. Analysis may be accomplished by mass spectrometry, dew point determination, or by the weighing the water and measuring the volume hydrogen per unit time. The flow meters must be calibrated in-line to determine the exact volume of gas passing through in a measured time. Nagasaka et al.(1994) used a Drierite-filled column to check the weight gain in every experimental run for measured water vapor pressures reigning from 0.002 to 0.3 atmosphere. The calculated water vapour pressure, if the oxygen activity is fixed by the Al/Al_2O_3-reaction, is much lower than the values reported by Nagasaka et al(1994), thus needing long adsorption times to yield measurable quantities of water.

Very low oxygen pressures, as in this study, can be obtained with the following dynamic methods:

- Saturation of hydrogen with water vapour by passing it over or through an ice bed
- By passing hydrogen through a saturated salt solution e.g.. Lithium chloride solution. (Chipman,1953)
- The amount of water vapour can be fixed by contacting the hydrogen gas with a sulphuric acid solution at a controlled temperature.
- Using the oxalic acid dihydrate/ oxalic acid equilibrium (Belton,1998)

The application of ice is limited by very slow kinetics and very intimate contact between the ice and the hydrogen gas must be obtained. A further drawback is difficulty in controlling and measuring the ice temperature to maintain a constant gas composition throughout an experimental run.

According to Belton(1998) early workers very precisely established the water vapor pressure of oxalic acid dihydrate / oxalic acid mixtures, and obtained

$$\text{Log P (mm Hg)} = 18.053 - 9661/(T + 250) \qquad (30)$$

With

T = Temperature (K)

At a temperature of 273K water/hydrogen ratios as low as 0.0005 can be conveniently obtained, using the oxalic acid dihydrate / oxalic acid equilibrium.

The application of sulphuric acid as solvent enables better temperature control by immersion of the contactors in a well stirred bath, but the constant removal of water from the sulphuric acid leads to the alteration of gas composition with time. The time dependence can be estimated by means of dynamic mass balance calculations

The partial water vapour pressure as a function of temperature and solution composition can be obtained by fitting curves to experimental data given in Perry et al (1985). The temperature-composition dependance of the partial water pressure, temperature range: 30 – 60 °C and 70 –85 % sulphuric acid solutions, is represented by the following equation.

$$P_{H2O}(bar) = (-3.372 + 0.2584\,T - 0.00616\,T^2 + 5.017*10^{-5}\,T^3) + (0.1449 - 0.011\,T + 2.628*10^{-4}\,T^2 - 2.122*10^{-6}\,T^3) * \%\,H_2SO_4 + (0.002068 + 1.569*10^{-4}\,T - 3.736*10^{-6}\,T^2 + 2.972*10^{-8}\,T^3) * (\%\,H_2SO_4)^2 + (9.8*10^{-6} - 7.4*10^{-7} * T + 1.7*10^{-8} * T^2 + 1.389 * 10^{-10}\,T^3) * ((\%\,H_2SO_4)^3 \quad (31)$$

with

T = Temperature (K)

Using this information and a simple mass balance, the change in solution composition with time can be estimated. This was performed by calculating the amount of water stripped out of the saturator for a given period assuming equilibrium between the water in the sulphuric acid and in the gas stream. The composition of the sulphuric acid was recalculated after each period. The calculations were repeated utilizing the new composition of the sulphuric acid and equation 31 to calculate the amount of water stripped out of the saturators for the next incremental period. The values used in this calculation, depicted in figure 20, are as follows

Initial sulphuric acid composition	80 %
Temperature of water bath	36 °C
Mass of solution	2025 g
Total pressure above contactor	0.87 atmosphere
Gas flow rate	0.18Nm^3/min
Equilibration temperature.	1700 °C

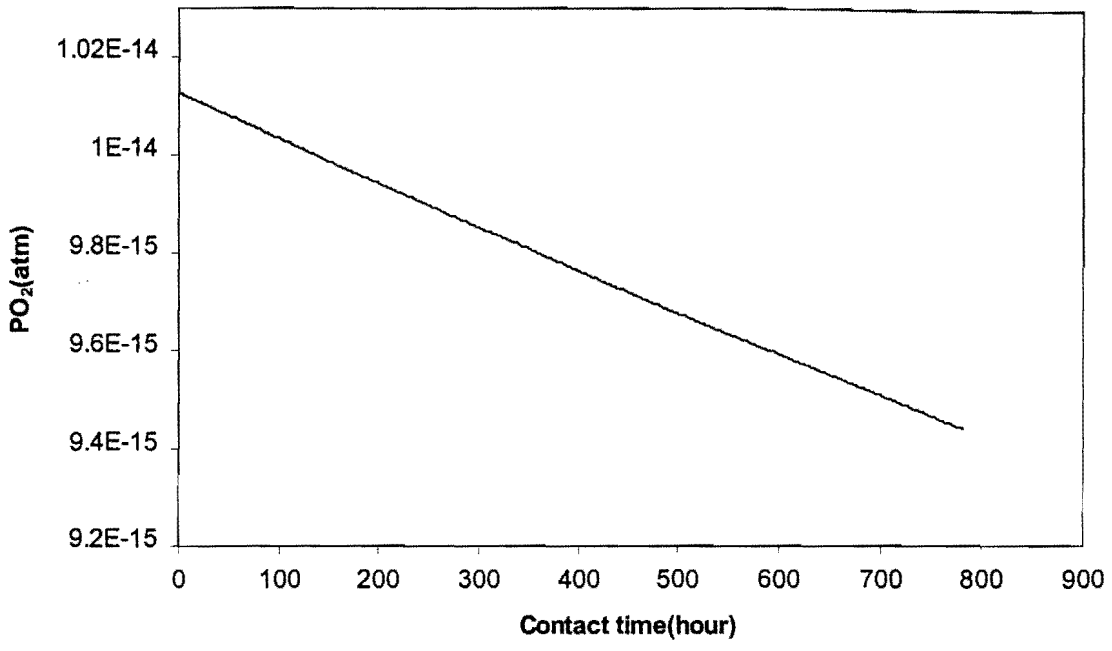

Figure 20: Calculated change of oxygen activity at 1700 °C for a H_2-H_2O mixture prepared with a 80 % sulphuric acid solution, for a hydrogen gas flow rate of 0.18Nm^3/min through an acid bath of 2025 g.

The figure depicts a 7.8 % change in the partial oxygen pressure for a 200 hour exposure period.

The effect of this change on the accuracy of the equilibrium measurements can be estimated as follows.

$$2V + 1.5\ O_2 = 2\ VO_{1.5} \qquad (32)$$

The vanadium oxide activity depends on the oxygen activity as follows

$$a_{VO1.5} \propto Po_2^{0.75} \qquad (33)$$

A variation of 7.8% in the oxygen activity thus yields an uncertainty of 4.7% in the vanadium oxide activity coefficient. This is expected to be well in the range of

experimental errors, indicating that the sulfuric acid needs only be replaced every 200 hours.

The temperature of the water bath in which the saturators are immersed should be carefully controlled because the water vapor pressure over the solvent depends exponentially on the temperature, as indicated by figure 21.

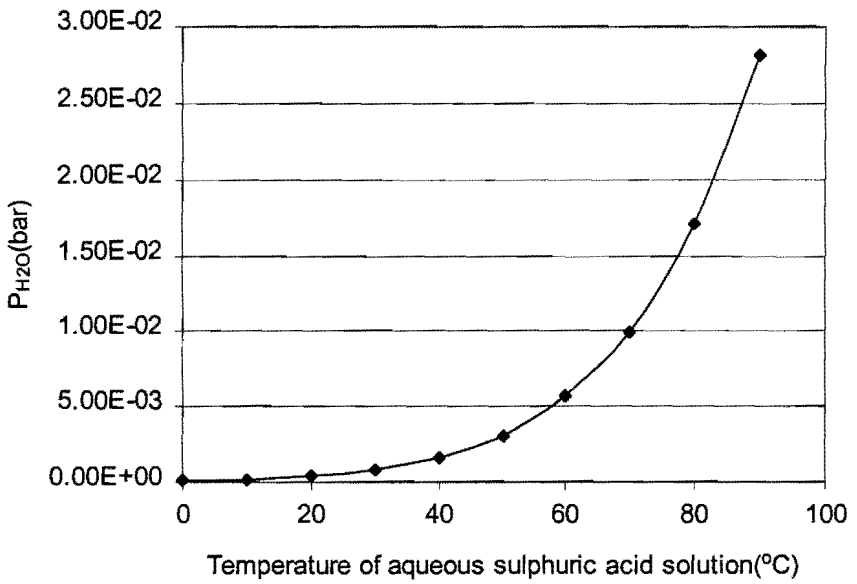

Figure 21: Effect of temperature on the partial water pressure above a 85 % sulphuric acid solution, (Perry,1985)

A circulating water bath with a controller will ensure uniform temperatures where a number of saturators are used in series. To prevent alteration of the gas mixture being used all the gas-carrying tubes must be heated to prevent condensation. Minu et al.(1948) reported tube temperatures around 80 °C, for a mole fraction water in the gas stream of 0.175, to prevent condensation.

All the adjustable parameters should be carefully controlled if accurate results are to be obtained.

1.5.3. Kinetics of the vanadium oxidation reaction

The overall reaction can be divided in a number of steps taking place in series. The first step is the mass transfer of H_20 as a gas across the boundary layer, to the gas-slag interface. The second step is the actual chemical reaction of H_20 at the the gas-slag interface by adsorption and reaction with the slag phase. The next step entails the mass transfer of the absorbed species to the slag-metal interface. Another chemical reaction takes place at this interface whereby vanadium is oxidized. The step following the oxidation reaction is the mass transfer of the vanadium oxide from the interface to the bulk of the slag, increasing the average vanadium content in the slag. The slowest of these steps will govern the overall rate of the overall reaction.

Chemical reactions are activation energy controlled remaining close to equilibrium at high temperatures. Thus mass transfer may be the rate-limiting step. The purpose of this discussion is to evaluate the mass transfer of water to the slag-gas interface as a possible rate-determining step. Unfortunately not much is known about the diffusion of vanadium species in slags.

If the rate of the overall reaction is determined by the rate of mass transfer of H_20 to the interface, then the rate of water vapor diffusion can be expressed according to the following reaction.

$$\frac{dN_{H_2O}}{dt} = m\,A\left(C_{H_2O}^{bulk} - C_{H_2O}^{inter}\right) \qquad (34)$$

The rate of vanadium oxidation(mol/hr) is 0.66 times the rate of mass transfer of H_20 to the interface In this equation $\frac{dN_{H_2O}}{dt}$ is the rate of mass transfer of H_20 to the interface and m is the mass transfer coefficient.

Assume $C_{H_2O}^{inter} = 0$ and P_{H_2O} is smaller than 0.1 atmosphere, (Nagasaka,1994), then

$$\frac{dN_{H_2O}}{dt} = \frac{m}{RT}\left(P_{H_2O}^{bulk}\right) \text{ (mol/cm}^2\text{s}^{-1}\text{)} \qquad (35)$$

With R the universal gas constant, T the temperature in K and $P_{H_2O}^{bulk}$ the partial water pressure of the bulk gas phase.

Assume the following oxidation isotherm for vanadium

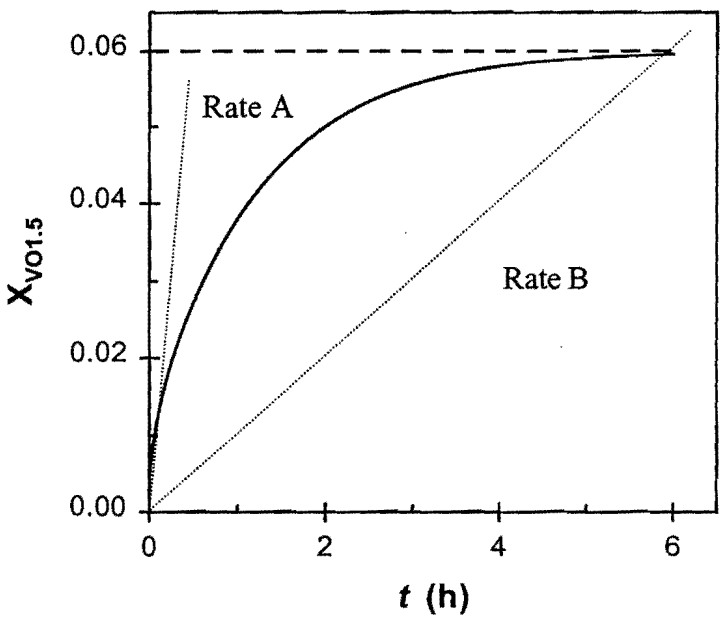

Figure 22: Assumed vanadium oxidation isotherm

Six hours is the assumed duration time for each experimental trial to reach equilibrium at a given temperature. It is further assumed (based on industrial slags) that the equilibrium mole fraction vanadium is 0.06. Two oxidation rates are now considered, Rate A (the initial rate) and Rate B (the average oxidation rate). See figure 22.

Fluid dynamics calculations for a specific experimental setup can evaluate the mass transfer coefficient(m) in equation 34. Mannion et al.(1991) and Nagasaka et al.(1993) used these equations to good effect to investigate gas mass transfer control in reactions where the chemical reactions were sufficiently fast. The experimental setup of this study, correlating with their studies, is as follows:

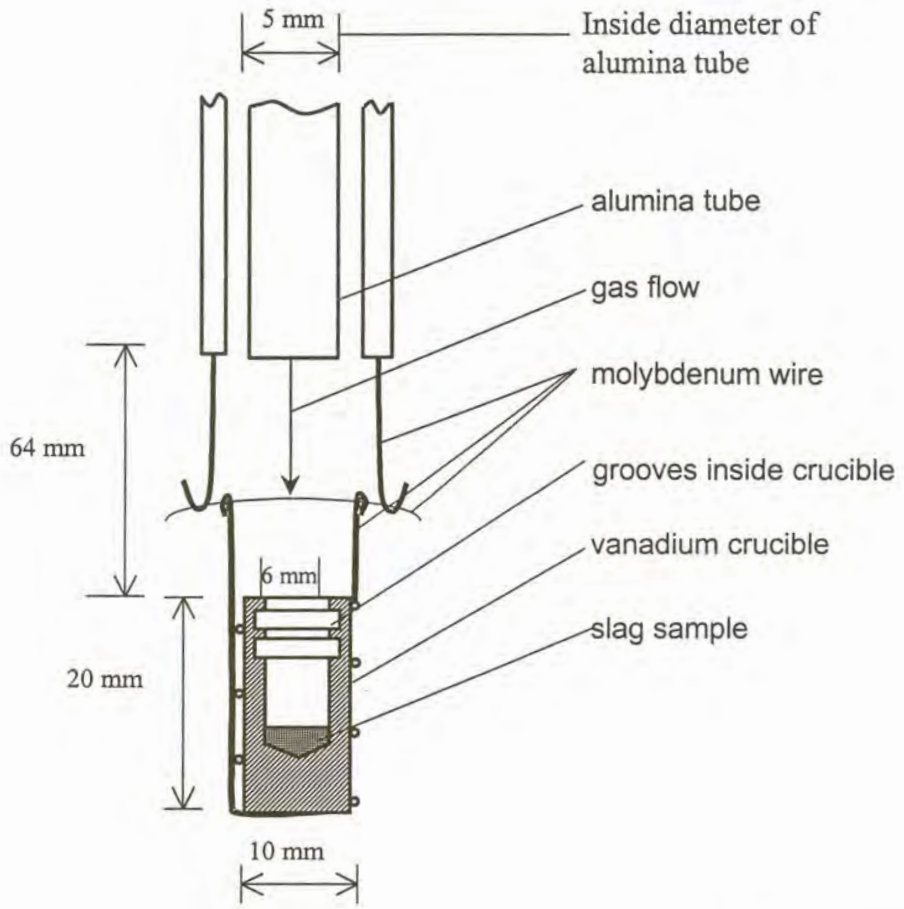

Figure 23: Planned configuration to suspend vanadium crucible inside the tube furnace.

The average mass transfer coefficient may be calculated using the following empirical equations. The Sherwood number (*Sh*) enables the calculation of the average mass transfer coefficient and was proposed to be as in equation 36, by Mannion(1992) and 37 by Nagasaka(1994).

$$Sh = 0.4(\pm 0.13)\left(\frac{d}{r}\right) Re^{0.66}\, Sc^{0.55} \qquad (36)$$

Or

$$Sh = 0.27(\pm 0.07)\left(\frac{d}{r}\right)^{1.5} Re^{0.76}\, Sc^{0.5} \qquad (37)$$

And

$$\mathrm{Sh} = m\frac{d}{D} \tag{38}$$

With

d = diameter of nozzle (m)

r = radius of crucible (m)

μ = viscosity (Pa.s)

ρ = density (kg/m^3)

D = interdiffusivity (m^2/s)

u = linear velocity (m/s)

m = mass transfer coefficient.(m/s)

Using the gas properties of interest the dimensionless Reynolds (*Re*) and Schmidt (*Sc*) numbers can now be calculated as in equation 39 and 40 respectively.

$$Re = \frac{du\rho}{\mu} \tag{39}$$

$$Sc = \frac{\mu}{\rho D} \tag{40}$$

Because of the low P_{H_2O} needed (see Table 10) the gas mixture can be considered to be pure H_2 and the gas properties of H_2 are shown in Table 11 for a gas temperature which is the average of the slightly preheated gas (330K) and the metal surface (1973-2123K).

Properties of H_2 (1200K)	
ρ	0.0176 kg/m^3 (calculated using ideal gas law)
μ	0.000024 Pa.s (Fruehan,1998)
D	9.97 *10^{-4} m^2/s (Szekely,1971)

Table 11: Properties of H_2 at 1200 K

The values used in the calculation are shown in Table 12

Values used in calculations	
Slag mass	0.0002 kg
Molar mass of slag (CaO: Al2O3 1:1)	0.079 kg/mol
Mole slag	0.00253 mol
Total pressure	0.876 atm
Bulk P_{H2O}	0.0004*101300 Pa

Table 12: Values of constants used to perform the calculations

In addition to the value of D reported by Perry et al.(1985) to be 9.97 cm^2/s, it may also be calculated using the empirical equation also proposed by Perry et al.(1985).

$$D_{AB} = \frac{10^{-3} T^{1.75} \left[\frac{(M_A + M_B)}{M_A M_B} \right]^{0.5}}{P\left[\left(\sum V_A \right)^{\frac{1}{3}} + \left(\sum V_B \right)^{\frac{1}{3}} \right]^2} \qquad (41)$$

where

T = temperature in K (1200K)

P = pressure in atmosphere

D = interdiffusivity

$M_A M_B$ = molar mass of specie A and B respectively.

$\sum V_A, \sum V_B$ = Atomic diffusion volumes

Table 13 shows atomic diffusion volumes of some of the gases found in metallurgical processing.

Specie	atomic diffusion volumes
H_2	7.07
N_2	17.9
O_2	16.6
Air	20.1
CO	18.9
CO_2	26.9
H_2O	12.7
SO_2	41.1

Table 13: Atomic diffusion volumes for use in estimating D_{AB} (Perry et al.,1985).

The gas diffusivity of H_20-H_2 was calculated to be 10.08 cm^2/s, at 1200 K, using equation 41.

The two correlations used to calculate the minimum gas flow rate needed to maintain the oxidation rates showed in figure 22, resulted in slightly different results as seen in Table 14.

		Mannion	Nagasaka
		Gas flow rates(ml/min)	Gas flow rates(ml/min)
Oxidation rate A	$1.41 * 10^{-7}$ mol/s	4015	5065
Oxidation rate B	$7.03 * 10^{-9}$ mol/s	43	54.2

Table 14: Results of fluid flow calculations for different oxidation rates. Flow rates are for 25 °C and 0.865 atm pressure.

Darken et al (1945) have established that approximately 0.9cm/s (10.6 ml/min through a tube, I.D. 5mm) is an optimum linear flow rate through a cylindrical tube to minimize thermal diffusion and temperature uncertainties.

It is evident from the results that very low flow rates are sufficient for an assumed oxidation rate if gas mass transfer is the rate-determining step (rate B). Thus, the gas mass

transfer does not have a profound effect on the kinetics of the oxidation rate and should therefore not be the rate determining step. One of the other reaction mechanisms proposed could therefore be rate limiting.

1.6. Conclusion

It can be concluded that the Al_2O_3 content of the slag (or slag basicity) has a strong effect on the amount of oxidic vanadium in the slag. In addition to this, the amount of vanadium in metallic form is also dependent on the slag basicity. Both of these mechanisms of vanadium loss to the slag should be quantified in order to maximize vanadium recovery. The oxidic vanadium loss to the slag can be quantified by performing high temperature equilibrium experiments utilizing hydrogen-water mixtures to fix the oxygen activity.